Published in final edited form as:
Neurobiol Aging. 2010 April ; 31(4): 549–566. doi:10.1016/j.neurobiolaging.2008.05.013.

Neuronal gene expression in non-demented individuals with intermediate Alzheimer's Disease neuropathology

Winnie S. Liang[a,b], **Travis Dunckley**[a,b], **Thomas G. Beach**[b,c], **Andrew Grover**[b,c], **Diego Mastroeni**[b,c], **Keri Ramsey**[a], **Richard J. Caselli**[b,d], **Walter A. Kukull**[e], **Daniel McKeel**[f], **John C. Morris**[f], **Christine M. Hulette**[g], **Donald Schmechel**[g], **Eric M. Reiman**[a,b,h], **Joseph Rogers**[b,c], and **Dietrich A. Stephan**[a,b,i,*]

[a]Neurogenomics Division, Translational Genomics Research Institute, Phoenix, AZ 85004, USA

[b]Arizona Alzheimer's Disease Consortium, Phoenix, AZ 85006, USA

[c]Sun Health Research Institute, Sun City, AZ 85351, USA

[d]Department of Neurology, Mayo Clinic, Scottsdale, AZ 85259, USA

[e]National Alzheimer's Coordinating Center, Seattle, WA 98105, USA

[f]Washington University Alzheimer's Disease Research Center, St. Louis, MO 63108, USA

[g]Duke University Alzheimer's Disease Research Center, Durham, NC 27705, USA

[h]Banner Alzheimer's Institute, Phoenix, AZ 85006, USA

[i]Navigenics, Redwood Shores, CA 94065, USA

Abstract

While the clinical and neuropathological characterization of Alzheimer's Disease (AD) is well defined, our understanding of the progression of pathologic mechanisms in AD remains unclear. Post-mortem brains from individuals who did not fulfill clinical criteria for AD may still demonstrate measurable levels of AD pathologies to suggest that they may have presented with clinical symptoms had they lived longer or are able to stave off disease progression. Comparison between such individuals and those clinically diagnosed and pathologically confirmed to have AD will be key in delineating AD pathogenesis and neuroprotection. In this study, we expression profiled laser capture microdissected non-tangle bearing neurons in 6 post-mortem brain regions that are differentially affected in the AD brain from 10 non-demented individuals demonstrating intermediate AD neuropathologies (NDAD; Braak stage of II through IV and CERAD rating of moderate to frequent) and evaluated this data against that from individuals who have been diagnosed with late onset AD as well as healthy elderly controls. We identified common statistically significant expression changes in both NDAD and AD brains that may establish a degenerative link between the two cohorts, in addition to NDAD specific transcriptomic changes. These findings pinpoint novel targets for developing earlier diagnostics and preventative therapies for AD prior to diagnosis of probable AD. We also provide this high-quality, low post-mortem interval (PMI), cell-specific, and region-specific NDAD/AD reference data set to the community as a public resource.

*Corresponding author at: Neurogenomics Division, The Translational Genomics Research Institute, 445 North Fifth Street, Phoenix, AZ 85004, USA. Tel.: +1 602 343 8727; fax: +1 602 343 8844.

Conflict of interest statement
The authors state that there are no actual or potential conflicts of interest.

Keywords

Laser capture microdissection; Affymetrix microarrays; Expression profiling; Neuron; Transcriptomics

1. Introduction

With its increasing incidence, Alzheimer's Disease (AD) has become a major concern for both the research community as well as the aging global population. Because identification of pathological markers is currently the only approach to confirming diagnosis, physicians and researchers have begun to focus on developing early diagnostic tools to allow for earlier preventative measures. One potential approach is to consider earlier stages of AD in which individuals do not demonstrate clinical criteria for AD dementia but may demonstrate intermediate levels of AD neuropathology (Braak stage of II, III, or IV with moderate to frequent neuritic plaques) evaluated post-mortemly. This characterization suggests that these individuals may have developed clinical AD symptoms had they lived longer, or are able to stave off disease progression. Evaluating such individuals compared to those who had been clinically diagnosed and histopathologically confirmed to have AD will help to elucidate the neuronal processes that may drive disease progression or neuroprotection. To begin to elucidate this putative relationship, we expression profiled laser capture microdissected non-tangle bearing cortical neurons from six functionally discrete post-mortem brain regions. These regions, which have been found to display differential susceptibilities to AD pathologies, were collected from 10 non-demented individuals that demonstrate intermediate levels of AD neuropathology (NDAD). This analysis builds upon the global neuronal expression resource (Liang et al., 2008) we have established focusing on healthy elderly controls and patients who had been diagnosed with late onset AD, and aims to provide a catalog of expression signatures that characterizes transcriptomic changes across control, NDAD, and AD brains.

The six regions profiled have differential susceptibilities to AD pathologies and include the entorhinal cortex (EC), hippocampus (HIP), middle temporal gyrus (MTG), posterior cingulate cortex (PC), superior frontal gyrus (SFG), and primary visual cortex (VCX). Based on analysis consolidating statistically significant gene expression changes in NDAD patients compared to controls and AD patients compared to controls, we have identified significant common expression changes in both NDAD and AD brains in addition to expression signatures that account for regional changes across NDAD and AD brains. These findings provide insight into pathogenic mechanisms that may link the progression from NDAD to AD in different parts of the human brain and also identifies novel targets for developing improved diagnostics and preventative therapeutics against AD.

2. Methods

2.1. Tissue collection

Brain samples were collected at two Alzheimer's Disease Centers (Washington University and Sun Health Research Institute) from clinically classified non-demented individuals who demonstrate intermediate levels of AD pathologies (6 males and 4 females) with a mean age of 86.6±5.3. Individuals were matched as closely as possible for their mean age at death and gender. Subjects in this group have a Braak stage of II to IV with a CERAD neuritic plaque density of moderate or frequent. Tissue collection from healthy elderly control and AD samples was previously described (Liang et al., 2008; Liang et al., 2007). Samples were collected (mean post-mortem interval (PMI) of 2.5 h) from six brain regions that are either histopathologically or metabolically relevant to AD—these include the EC (BA 28 and 34), SFG (BA 10 and 11),

HIP, VCX (BA 17), MTG (BA 21 and 37), and the PC (BA 23 and 31). Following dissection, samples were frozen, sectioned (8 μm), and fixed on glass slides.

Brain sections were stained with a combination of Thioflavin-S (Sigma; Dallas, TX) and 1% Neutral Red (Fisher Scientific; Chicago, IL) and pyramidal neurons were identified by their characteristic size, shape, and location within the region of interest, while tangles were identified by the fluorescence of Thioflavin-S staining. In the EC, the large stellate neurons lacking Thioflavin-S staining were collected from layer II and pyramidal cells lacking Thioflavin-S staining were collected from CA1 of the HIP. The CA1 region was selected for study because this area is the most affected and earliest affected region in the hippocampus in terms of tangle formation, and this region has already been expression profiled in neurologically healthy elderly individuals. In all other regions, cortical layer III pyramidal neurons lacking Thioflavin-S staining were collected (for all collected neurons, cell bodies were extracted). For each individual, approximately five hundred histopathologically normal pyramidal neurons were collected from the EC, HIP, MTG, PC, SFG, and VCX using LCM with the Arcturus Veritas Automated Laser Capture Microdissection System (Mountain View, CA). Cells were collected onto Arcturus CapSure Macro-LCM Caps and extracted according to the manufacturer's protocol. Total RNA was isolated from the cell lysate using the Arcturus PicoPure RNA Isolation Kit with DNase I treatment using Qiagen's RNase-free DNase Set (Valencia, CA).

2.2. Expression profiling

Expression profiling, hybridization, and array scanning was performed as previously described (Liang et al., 2008; Liang et al., 2007). Isolated total RNA from each sample of ~500 neurons was double round amplified, cleaned, and biotin-labeled using Affymetrix's GeneChip Two-Cycle Target Labeling kit (Santa Clara, CA) with a T7 promoter and Ambion's MEGAscript T7 High Yield Transcription kit (Austin, TX) as per manufacturer's protocol. Amplified and labeled cRNA was quantitated on a spectrophotometer and run on a 1% TAE gel to check for an evenly distributed range of transcript sizes. Twenty micrograms of cRNA was fragmented to approximately 35–200 bp by alkaline treatment (200 mM Tris-acetate, pH 8.2, 500 mM KOAc, 150 mM MgOAc) and run on a 1% TAE gel to verify fragmentation. Separate hybridization cocktails were made using 15μg of fragmented cRNA from each sample as per Affymetrix's protocol.

Two hundred microliters (containing 10μg of fragmented cRNA) of each cocktail was separately hybridized to an Affymetrix Human Genome U133 Plus 2.0 Array for 16h at 45°C in the Hybridization Oven 640. The Affymetrix Human Genome Arrays measure the expression of over 47,000 transcripts and variants, including 38,500 characterized human genes. Arrays were washed on Affymetrix's upgraded GeneChip Fluidics Station 450 using a primary streptavidin phycoerythrin (SAPE) stain, subsequent biotinylated antibody stain, and secondary SAPE stain. Arrays were scanned on Affymetrix's GeneChip Scanner 3000 7G with AutoLoader. Scanned images obtained by the Affymetrix GeneChip Operating Software (GCOS) v1.2 were used to extract raw signal intensity values per probe set on the array. MAS5.0 was used to calculate detection calls (absent, marginal, or present) and to scale all raw chip data to 150 to normalize signal intensities for inter-array comparisons. Reports generated by GCOS were reviewed for quality control—we looked for at least 20% present calls, a maximum 3′/5′ GAPDH ratio of 30.5, and a scaling factor under 11. Thirteen arrays that failed to pass these standards were not included in further analyses.

2.3. Pyramidal cell quality control

To ensure neuronal cell purity in the samples, expression of GFAP, an astrocyte cell marker, was evaluated. Five samples that had GFAP expression greater than 2 S.D. from the mean were removed from statistical analyses.

2.4. Statistical analysis

Data for samples from neurologically healthy elderly controls and AD-afflicted individuals were generated in previous studies (Liang et al., 2008; Liang et al., 2007). Microarray data files of the normal samples are available on the Gene Expression Omnibus (GEO) site at http://www.ncbi.nlm.nih.gov/geo/query/acc.cgi?acc=GSE5281 (project accession#GSE5281) and regional analyses are posted at http://www.tgen.org/neurogenomics/data/). A summary of the mean ages, gender numbers, and number of samples used for statistical analyses (across all groups) are shown in Table 1. As a metric of quality, *R*-squared values were calculated and averaged for each region within each sample group—these values are posted on the supplementary data site at http://www.tgen.org/neurogenomics/data.

Direct comparisons between brains of neurologically healthy and NDAD brains were performed between all brain regions to analyze expression differences. For each analysis, genes that did not demonstrate at least approximately 10% present calls for each region-specific comparison were removed using Genespring GX 7.3 Expression Analysis software (Agilent Technologies; Palo Alto, CA). A two-tailed unpaired *t*-test, assuming unequal variances (with multiple testing corrections using the Benjamini and Hochberg False Discovery Rate (FDR)), was applied to each comparison in Excel to locate genes that are statistically significant in differentiating expression between healthy and NDAD brains: for each analysis, genes that had a maximum *P*-value of 0.01 were collected and those genes whose average NDAD signal and average control signal were both below a threshold of 150 were removed. Fold change values were determined by calculating the ratio between the average scaled expression signal (for all samples) for a gene from the NDAD sample region and the average scaled expression signal for the same gene from the normal samples.

Using this approach we identified sets of genes that were specifically up or down-regulated between normal and NDAD brains for each of the six brain regions-of-study. Maps for genes showing the greatest statistically significant ($P < 0.01$, corrected) changes in the NDAD versus controls analysis were assembled. For the EC, a minimum (increased or decreased) fold change of 6 was applied, for the HIP a 5.4-fold change, for the MTG an 6.2-fold change, for the PC a 4-fold change, for the SFG a 4.8-fold change, and for the VCX a 2.9-fold change. Heat maps for each brain region were created using GeneCluster v2.0 with no gene or sample clustering applied and are located on a supplementary data site at http://www.tgen.org/neurogenomics/data.

To find common statistically significant expression changes in AD and NDAD brains, each regional analysis ($P < 0.01$ with multiple testing corrections) for NDAD cases versus controls was compared against the parallel regional analysis for AD versus controls (Liang et al., 2008). Genes showing the greatest fold changes from the intersection lists were used to generate heat maps with GeneCluster v2.0 (Reich et al., 2004) (Fig. 1). For the EC, a minimum (increased or decreased) fold change of 5.0 was applied (for both the NDAD versus control analysis and AD versus control analysis), for the HIP a 4.3-fold change, for the MTG an 4.5-fold change, for the PC a 2.5-fold change, for the SFG a 3.0-fold change, and for the VCX a 1.8-fold change. To evaluate NDAD-specific alterations, genes showing statistically significant ($P < 0.01$ with corrections applied) expression changes only in the NDAD analyses, and not the AD analyses, were identified. Analyses are posted on the supplementary data site at http://www.tgen.org/neurogenomics/data/.

To identify expression patterns that account for the greatest amount of variance across disease states (healthy controls, NDAD, and AD) in each region, principle components analysis (PCA) was applied. PCA reduces a multi-dimensional data set to two dimensions by performing covariance analysis across the three sample groups. Genes showing at least ~10% present calls for each region were input into Genespring GX 7.3 for PCA analysis. For each region, three principle components were identified (the number of components is determined by the number of sample groups). The first component accounts for the greatest amount of variance across healthy control, NDAD, and AD brains, while the third component accounts for the least amount of variance. For each component, correlation values are measured for each gene in the input list—correlation values range from 0 to 1 with a value of 1 indicating that the gene has an identical expression signature to the specific component. Genes demonstrating a correlation value of 1 to component 1 for each region are listed in Table 5 and regional component graphs are shown in Fig. 2—the percentage of expression variance accounted for by each component is shown. Additional correlation data is listed on the supplementary data site.

2.5. Data posting

MIAME-compliant microarray data files are located on the Gene Expression Omnibus (GEO) site at http://www.ncbi.nlm.nih.gov/geo/query/acc.cgi?acc=GSE5281 (project accession#GSE5281). Fold change and *P*-value data for each of the six regions across healthy control, NDAD, and AD brains are available online at: http://www.tgen.org/neurogenomics/data/. Posted lists show region-specific *P*-values and fold changes, and expression signals for genes that have at least approximately 10% present calls across regional samples with a maximum *P*-value of 0.01 with multiple testing corrections applied (no fold change thresholds have been applied on these lists).

2.6. RT-PCR validation of neuron-specific candidate genes

Total RNA was isolated from cortical grey matter from unprofiled MTG (controls: $n = 9$, NDAD cases: $n = 8$, AD cases: $n = 9$) and PC (controls: $n = 8$, NDAD cases: $n = 8$, AD cases: $n = 11$) frozen tissue using the RNAspin Mini kit (GE Healthcare Life Sciences; Piscataway, NJ) using manufacturers protocol modified by increasing initial volume of buffer RA1 to 500 µl to prevent subsequent column blockage. RNA quality was assessed on an Agilent 2100 Bioanalyzer (Santa Clara, CA) using Agilent RNA Nanochips. RIN numbers of 6.5 (range 6.5–9.0) and above were considered sufficient for this analysis. cDNA was generated using the Superscript First Strand Synthesis kit (Invitrogen; Carlsbad, CA) using 1 µg of total RNA in a 40 µl reaction. Quantitative RT-PCR was performed using Taqman primer/probe sets (Applied Biosystems; Foster City, CA) to amplify the following neuron-specific gene transcripts; MAP1B (microtubule-associated protein 1B; Hs00195485_m1), GRIA1 (glutamate receptor, ionotropic, AMPA 1; Hs00181348_m1) and GRIA3 (glutamate receptor, ionotropic, AMPA 3; Hs00241485_m1). Five assays for non-neuronal mRNA transcripts were performed, of which the first four are AD-related; APOE (apolipoprotein E; Hs0003037354_mH), APP (amyloid precursor protein; Hs00169098_m1), BACE1 (beta-site APP-cleaving enzyme 1; Hs00201573_m1), COX5B (cytochrome c oxidase subunit Vb; Hs00426948_m1) and MAP4 (microtubule-associated protein 4; Hs01104794_m1). Levels of β-Gluconuridase (GUSB 4333767F) mRNA were used for normalization of samples; this gene transcript did not show significant expression changes between AD and ND in the gene array analysis, and has been successfully employed for this purpose previously (Barrachina et al., 2006; Kuwano et al., 2006). qRT-PCR reactions were performed in 30 µl reactions using Taqman Gene Expression Master Mix (Applied Biosys-tems) according to manufacturers protocol on a BioRad iCycler IQ qPCR system (Hercules, CA). Threshold values were calculated using the maximum curvature approach. Ct values were used to calculate fold changes using the $2^{-\Delta\Delta Ct}$ method (Livak and Schmittgen, 2001). Significance of observed changes was ascertained using the Student's *t*-test.

3. Results and discussion

In this study, we gene expression profiled non-tangle bearing cortical neurons from the post-mortem brains of non-demented individuals who have been histopathologically confirmed to demonstrate intermediate pathologies associated with AD through Braak and CERAD staging. This study completes a high-quality expression data set that we have established to evaluate neuronal gene expression changes that characterize healthy elderly controls, non-demented individuals with intermediate AD neuropathology, and AD patients in different areas of the brain that are relevant to AD. By defining neuronal expression levels across healthy elderly individuals, NDAD individuals, and those diagnosed with late-onset AD, these findings provide insight into disease progression and the processes that may drive neurodegeneration or neuropro tection.

3.1. Common expression changes in NDAD and AD brains

In order to identify common expression changes in NDAD and AD brains, we compared our data with our previous study in which we similarly profiled neurons from the brains of healthy elderly controls and individuals that have been clinically and histopathologically confirmed to have AD (Liang et al., 2008). Comparison of expression changes in NDAD versus control brains and AD versus control brains led to the identification of a significant overlap of genes demonstrating statistically significant ($P < 0.01$, corrected for multiple comparisons) expression changes within each regional analysis. In the EC, 1887 genes showed significant changes in both NDAD and AD brains compared to controls, 1892 genes demonstrated changes in the HIP of both NDAD and AD brains, 2755 genes in the MTG, 503 genes in the PC, 226 genes in the SFG, and 178 genes in the VCX. Interestingly, the SFG, a region that demonstrates metabolic changes associated with normal aging (Angelie et al., 2001; Convit et al., 2001; Ivancevic et al., 2000; Loessner et al., 1995; Moeller et al., 1996), and the VCX, a region found to be relatively spared from AD pathologies (Metsaars et al., 2003), showed the least amount of transcriptomic changes across healthy elderly, NDAD, and AD brains, while the greatest changes were found in brain regions that have increased susceptibilities to AD pathologies including neurofibrillary tangles (NFTs) (Bobinski et al., 1999; Bouras et al., 1994; Braak and Braak, 1992; de Leon et al., 1989; Du et al., 2003; Fox et al., 1996; Frisoni et al., 1999; Hyman et al., 1984) in the EC and HIP, and amyloid plaques (Braak and Braak, 1991; Mirra et al., 1991; Thal et al., 2002) and metabolic deficits (Blesa et al., 1996; Jack et al., 1998; Mielke et al., 1994, 1998; Small et al., 2000) in the MTG and PC. Dendrograms listing genes demonstrating the greatest expression changes in both NDAD and AD brains compared to controls for each region are shown in Fig. 1.

Due to the breadth of the data, we focused our attention on genes that have roles in mechanisms that have been previously implicated as being associated with AD to assess if these pathogenic pathways may be enacted in NDAD brains. These mechanisms include pathways leading to formation of NFTs and amyloid plaques, ubiquitin–proteasomal pathways, and pathways surrounding synaptic degeneration.

3.1.1. Common expression changes in NDAD and AD brains: tangle and plaque related pathways—With regards to pathological markers of AD, NFTs form as a result of intraneuronal aggregation of tau, while extracellular plaques form as a result of the aggregation of insoluble 40–42 amino acid long Abeta proteins. In the EC and MTG, decreased expression was identified for microtubule-associated protein tau (MAPT) across NDAD and AD brains (Table 2), while multiple probes in the HIP demonstrated both increased and decreased expression. Past studies have identified isoform specific (3-repeat and 4-repeat) tau expression in the temporal region (Conrad et al., 2007) and cerebellar cortex (Boutajangout et al., 2004), and in cholinergic basal forebrain and hippocampal CA1 neurons of AD brains (Ginsberg et

al., 2006). However, the Affymetrix Human Genome U133 Plus 2.0 array does not specifically distinguish between 3-repeat and 4-repeat tau isoforms so that isoform-specific expression is not considered in this study. Even so, because of the presence of multiple probes targeted against MAPT, differences in expression changes between probes suggest that isoform-specific expression is present. In the HIP, 3 MAPT probes demonstrated significant opposite changes in expression levels in NDAD brains (Table 2). While 206401_s_at and 203928_x_at target the entire length of MAPT and demonstrate increased expression, 225379_at targets the 3′ untranslated region (UTR) and demonstrates decreased expression. Because 206401_s_at and 203928_x_at cover the entire MAPT gene, including alternatively spliced exons, their changes in expression may represent differential expression of different isoforms. Because 225379_at targets the 3′ UTR, this probe evaluates all variants and thus likely represents the net change in expression of MAPT. While isoform-specific expression changes have been identified in AD brains, past studies have not found changes in MAPT expression in post-mortem brain tissue (Goedert et al., 1989) and single cells in AD (Hemby et al., 2003). Another study evaluated gene expression differences in tangle bearing hippocampal CA1 neurons from AD brains compared to non-tangle bearing CA1 neurons in both AD brains and healthy brains and did not detect any expression changes of the 3-repeat and 4-repeat isoforms (Ginsberg et al., 2000). However, in this particular study, gene expression of non-tangle bearing neurons from AD and control brains defined the baseline of expression so that disease specific changes in healthy neurons are not evaluated. Despite these findings, we identified changes in MAPT expression between healthy neurons in NDAD brains and healthy neurons in control brains (to parallel greater expression changes in healthy neurons in AD brains compared to that in control brains). The primarily decreased net expression of MAPT across control, NDAD, and AD brains found here may demonstrate cellular efforts to inhibit aggregation of tau into NFTs at a timepoint prior to onset of measureable cognitive deficits.

Cellular efforts to inhibit NFT formation may also be demonstrated by decreased expression of kinases that can phosphorylate tau—these include MAP/microtubule affinity-regulating kinases (MARK3, MARK4), cyclin-dependent kinase 5 (CDK5), PTEN-induced putative kinase 1 (PINK1), and tau tubulin kinase 2 (TTBK2) (Kitano-Takahashi et al., 2007) (Table 2). Along with decreases, increased expression for putative tau kinases were also identified (Table 2). The decreased expression of tau in certain regions along with altered expression of kinases that may phosphorylate tau suggests that neurons may be initiating responses to lessen or inhibit tangle formation at stages prior to detectable disease onset.

Evaluation of relevant factors in plaque formation pathways also led to the identification of altered expression of beta-secretase (BACE1), presenilins 1 and 2 (PSEN1, PSEN2), and APP (Table 2). Decreased expression was found for BACE1, the enzyme that makes the initial cleave in APP during sequential processing to generate Abeta proteins (Selkoe, 2001;Selkoe and Schenk, 2003;Sinha et al., 1999;Vassar et al., 1999;Yan et al., 1999), in NDAD and AD brains (compared to controls). In contrast, another study focusing on the temporal neocortex identified an absence of BACE expression changes between AD and control brains (Matsui et al., 2007)—this difference may be derived from the earlier degenerative timepoint considered in this study as well as the cellular specificity of this study. Furthermore, presenilins 1 and 2, components of the gamma secretase complex, showed decreased expression (Table 2). In contrast, in AD brains, PSEN1 demonstrated increased expression in the temporal neocortex (Matsui et al., 2007). Lastly, APP demonstrated increased expression (Table 2) to possibly correlate with the moderate to frequent CERAD ratings assigned for the profiled NDAD and AD brains. However, other studies have shown varied results regarding APP mRNA levels in AD brains. While one study identified increased levels of APP isoforms containing a Kunitz-type serine protease inhibitor domain in the cerebral cortices of AD brains (Preece et al., 2004), another study also identified this trend but did not find changes in overall levels of APP mRNA in the temporal neo-cortices of AD and control brains (Matsui et al., 2007). In contrast,

Johnston et al. (1996) identified reductions in total APP mRNA levels in the mid-temporal cortices of AD brains. Although our APP expression findings contrast with these previous studies (and although we were unable to differentiate between APP mRNA isoforms on the Affymetrix array), it has been shown that APP expression differs greatly across subjects and thus may contribute to the differences found (Harrison et al., 1996;Oyama et al., 1991, 1993;Robinson et al., 1994). Additionally, as results from APP expression studies may differ, we considered both NDAD and AD cases and focused on neuron-specific regional expression to differentiate the findings presented here from whole tissue studies. The changes identified here suggest that common pathogenic or neuroprotective mechanisms are enacted in both NDAD and AD brains with regards to plaque formation. It is also particularly interesting to note the absence of significant expression alterations of NFT and plaque formation elements in the SFG and VCX, regions that are more spared from the hallmark AD pathologies.

3.1.2. Common expression changes in NDAD and AD brains: ubiquitin–proteasomal pathways—The toxicity of protein aggregates in the form of NFTs and plaques may also be related to changes or deficits in the ubiquitin–proteasomal pathway, a primary avenue for protein degradation. Across NDAD and AD brains and across all profiled regions, elements in the ubiquitin–proteasomal pathway showed both up-regulated and down-regulated expression with the lowest number of affected elements in the SFG and VCX. Altered expression was identified for ubiquitins (UBB, UBC), ubiquitin-conjugating enzymes (UBE1C, UBE1DC1, UBE2D2, UBE2D3, UBE2H, UBE2I, UBE2J1, UBE2L3, UBE2R2), ubiquitin specific peptidases (USP1, USP2, USP4, USP6-8, USP10, USP11, USP16, USP21, USP22, USP31, USP33, USP34, USP36, USP37, USP42, USP46-48, USP50, USP53, USP54), and proteasomal sub-units (PSMA1, PSMA5-7, PSMB1-7, PSMB10, PSMC1-3, PSMC5, PSMD1, PSMD4, PSMD11). The EC, SFG, and VCX showed solely decreased expression in NDAD and AD brains, while the HIP, MTG, and PC showed both increased and decreased expression for different subunits. Such dysregulated expression of ubiquitin–proteasomal pathway components indicates that this pathway is altered in NDAD and AD brains and may represent neuroprotective or pathogenic efforts (particularly with regards to the formation of plaques and tangles) that may begin at NDAD stages and potentially progress to AD.

3.1.3. Common expression changes in NDAD and AD brains: loss of synaptic connections—Another characteristic marker of AD is brain atrophy and loss of synaptic connections. To assess relevant expression changes that may affect such degeneration, we evaluated genes encoding synaptic proteins. These proteins include synaptosomal-associated protein, 25kDa (SNAP25), syntaxins (STX), synapsins (SYN), synap-tobrevins (vesicle-associated membrane protein; VAMP), synaptogyrins (SYNGR), and synaptotagmins (SYT) (refer to Table 3). SNAP-25, STX, and VAMP make up the SNARE complex, whose assembly allows for synaptic exocytosis (Sollner et al., 1993) and thus influences inter-neuronal communications. SYNs are phosphoproteins that help to regulate neurotransmitter release (Hackett et al., 1990;Hilfiker et al., 1998;Jovanovic et al., 2001,2000;Li et al., 1995;Llinas et al., 1985,1991;Rosahl et al., 1995) and also may have roles in establishing synaptic contacts. Finally, SYNGRs are suggested to be involved in vesicle exocytosis and membrane trafficking (Belizaire et al., 2004;Janz et al., 1999;Sugita et al., 1999), while SYTs are synaptic vesicle proteins that act as calcium sensors to support fast exocytosis and neurotransmitter release (Saraswati et al., 2007). Both up-regulated and down-regulated expression was identified for these synaptic factors (Table 3) to indicate drastic changes in demand for these proteins. In addition, increased expression of SYNs has been found to be correlated with establishing synaptic contacts (Ferreira et al., 2000;Lohmann et al., 1978;Melloni and DeGennaro, 1994) to suggest that the increased and decreased expression seen in this study may be correlated with a loss and establishment of synaptic contacts in NDAD brains. Such changes in contacts may ultimately lead to deficits in synaptic functions if contacts are not properly re-established.

3.2. Unique expression changes in NDAD brains

In addition to significant common expression changes in NDAD brains and AD brains compared to controls, unique statistically significant ($P < 0.01$, corrected) expression changes in NDAD brains (and absent or not significant in AD brains) were also identified. Pathway analysis using MetaCore GeneGo identified processes that contain these uniquely expressed genes. Data for these genes and all processes for each regional analysis are located on the supplementary data site. Interestingly, learning and/or memory processes were found to be affected in the EC, HIP, MTG, PC, and SFG of NDAD brains. Down-regulated genes from these processes include APOE, CHST10 (carbohydrate sulfotransferase 10), CTNND2 (catenin, delta 2), EGR1 (early growth response 1), ABI2 (Abl interactor 2), FYN (FYN oncogene), GM2A (GM2 ganglioside activator), PRKCB1 (protein kinase C, beta 1), PTN (pleiotrophin), S100B (S100 calcium binding protein, beta), and SHC3 (SHC transforming protein 3) (refer to Table 4). Up-regulated genes from learning and/or memory processes include ABI2, EFNB2 (ephrin-B2), MAPT, GRM7 (glutamate receptor, metabotropic 7), LAMB1 (laminin, beta 1), PRKACB (protein kinase, cAMP-dependent, catalytic, beta), and VDAC3 (voltage-dependent anion channel 3). While the NDAD patients did not meet clinical criteria for dementia, these transcriptomic changes precede stages during which dementia symptoms are detectable and may represent compensatory efforts targeted against onset of cognitive deficits. These learning/memory genes may thus represent novel factors to consider in developing earlier diagnostics and treatments.

Regional analysis of unique expression changes also identified additional affected pathways including cell communication (in the EC), neuron recognition (EC), neurite development (EC), cell organization and biogenesis (EC, HIP, PC, VCX), synaptic transmission (HIP, PC), regulation of neurotransmitter levels (HIP), intracellular transport (HIP, MTG, PC, VCX), smooth ER calcium ion homeostasis (MTG), neurophysiological process (PC), and negative regulation of apoptosis (SFG). Interestingly, in the VCX, the region found to be most spared from AD pathologies, the majority of the top processes include metabolic (protein, primary, cellular, macromolecule) and biosynthesis pathways, which may lend insight into earlier events that may influence this region's protection from plaque and tangle formation. While the implications for these process-specific changes are not clear, this analysis provides evidence of specific changes in NDAD brains apart from AD brains that may define an early timepoint in neurodegeneration.

3.3. Regional expression variance across sample groups

To consider a more global perspective of expression changes across the control, NDAD, and AD sample groups, principle components analysis (PCA) was applied for each region. This analysis evaluates expression levels across all three sample groups and pinpoints expression patterns (also referred to as components) that account for the greatest amount of expression variance across these groups. The components identified from this analysis, along with the percentage of variance accounted for by each component, are shown in Fig. 2. Those genes that demonstrate a signature identical to the first component (with a correlation value of 1), and thus demonstrate the greatest expression changes across the three sample groups, are listed in Table 5. Briefly, for the EC, HIP, and PC, component 1 for each of these regions demonstrates an overall decrease in expression levels across control, NDAD, and AD brains. In contrast, for the MTG, SFG, and VCX, component 1 for these regions demonstrates an increase in expression levels across control, NDAD, and AD brains.

Evaluation of the genes accounting for the greatest amount of expression changes within each region and across the three sample groups led to the identification of potentially biologically relevant factors in AD pathogenesis. The first is cathepsin D (CTSD), a gene that has been suggested to demonstrate a genetic association with AD risk and pathogenesis (Davidson et

al., 2006; Mariani et al., 2006; Papassotiropoulos et al., 2000) and which codes for a protease that may cleave apoE to generate fragments found in plaques (Zhou et al., 2006). CTSD, correlating with component 1 in the EC, demonstrates a decrease in expression starting from control brains, to NDAD brains, and to AD brains—this trend may represent neuroprotective efforts to inhibit plaque formation. Genes coding for enzymes that have primary roles in the ubiquitin–proteasomal pathway also demonstrated this downward trend across healthy brains to NDAD brains and to AD brains. These genes include UBR1 (ubiquitin protein ligase E3) which correlates with EC component 1 and UBE2I (ubiquitin-conjugating enzyme E2I), which correlates with PC component 1. These UBR1/UBE2I signatures suggest that their degradative pathways may be operating at lower levels in NDAD brains and more so in AD brains. Such down-regulation may represent a weakening of the ubiquitin–proteasomal system to ultimately allow buildup of NFTs. Also correlating with EC component 1 is neurexin 1 (NRXN1), whose transcripts can be alternatively spliced to generate alpha or beta isoforms. Interestingly, beta-neurexins interact with neuroligins to form and stabilize synapses (Benson et al., 2001; Scheiffele, 2003; Waites et al., 2005) so that the decreasing levels of expression shown by EC component 1 parallels characteristic loss of synaptic connections in AD brains and potentially in NDAD brains to a lesser extent.

PCA analysis of HIP also identified a number of interesting genes that correlate with component 1 in this region. First is CCS (copper chaperone for superoxide dismutase), which binds copper and complexes with and activates superoxide dismutase 1 (SOD1) (Brown et al., 2004; Culotta et al., 1997; Furukawa et al., 2004; Rae et al., 2001; Rothstein et al., 1999; Schmidt et al., 1999), an enzyme responsible for destroying free radicals. As AD pathogenesis is suggested to be influenced by oxidative stress resulting from free radicals (Markesbery, 1997), the expression signature for component 1 indicates a decrease in expression of CCS from healthy control brains to NDAD brains and to AD brains. This gradual decrease may demonstrate weakened neuronal efforts directed at fighting free radical toxicity in NDAD and AD brains. Second is ABAD (3-hydroxyacyl-CoA dehydro-genase type II), which has been found to be up-regulated in affected neurons in AD (Yan et al., 1997) and has been found to link Abeta to mitochondrial toxicity in AD (Lustbader et al., 2004). While HIP component 1 indicates a decrease in expression in NDAD and AD brains compared to controls, this finding correlates with our profiling of non-tangle bearing neurons. Also correlating with HIP component 1 is CAPNS1 (calpain, small subunit 1), which codes for a subunit common to all calpains. Increased activity of calpain has been suggested to be involved in AD development due to its association with perturbed calcium homeostasis (LaFerla, 2002; Mattson and Chan, 2003; Nixon, 2003; Vanderklish and Bahr, 2000). Thus, across NDAD and AD brains, the decreased expression of CAPNS1 may represent neuroprotective efforts enacted in healthy neurons of NDAD and AD brains.

Overall, PCA analysis identifies the expression trends within each region profiled and provides a general overview of region-specific transcriptomic changes that may be associated with disease progression. In the EC, HIP, and PC, significant down-regulation of gene expression is prevalent across control, NDAD, and AD brains, whereas in the MTG, SFG, and VCX, significant up-regulation of gene expression is seen. While further studies are necessary to decipher the implications of these changes, it is apparent that region-specific transcriptomic changes occur across brains of healthy elderly individuals, non-demented individuals with intermediate AD neuropathology, and clinically diagnosed AD patients with AD neuropathology, and may be key in understanding the timeline of AD pathogenesis.

3.4. RT-PCR validation of selected genes

To validate gene expression changes in NDAD brains, we performed RT-PCR on unprofiled fresh frozen brain sections from additional healthy elderly controls, NDAD cases, and AD

cases. Based on the NDAD analyses, genes were selected for validation based on statistical significance ($P < 0.05$, corrected), relevance to AD, and availability of brain tissue. Based on these criteria, GRIA1, GRIA3, MAP1B, APOE, APP, BACE1, COX5B, and MAP4 were evaluated in the MTG and APOE, APP, BACE1, COX5B, and MAP4 were evaluated in the PC. Results from RT-PCR analysis, along with the respective array data, are shown in Table 6 and Fig. 3.

In the MTG, RT-PCR data validated expression changes in NDAD brains compared to healthy elderly control brains for GRIA1, APOE, BACE1, COX5B, and MAP4 (all demon-strated decreased expression in NDAD brains compared to controls). Non-significant changes were identified for MAP1B and opposite (down-regulated) changes were found for APP. Furthermore, RT-PCR analysis of AD MTG samples compared to control samples validated down-regulated expression changes for GRIA1, MAP1B, and COX5B. In the PC, RT-PCR data also validated expression changes in NDAD brains compared to controls for APOE, BACE1, and COX5B (these genes all showed down-regulated expression in NDAD brains compared to controls), while opposite changes were identified for APP and MAP4. Along with the NDAD validation, RT-PCR also validated down-regulated AD versus control expression changes in the PC for APOE and COX5B, while APP and MAP4 demonstrated non-significant changes. This RT-PCR data provides independent validation of the majority of expression changes of relevant genes selected from array analysis of the MTG and PC.

4. Summary

In this study, we expression profiled non-tangle bearing neurons from the post-mortem brains of non-demented individuals who demonstrated median levels of AD pathologies in the brain. The findings we present here build upon our previous study in which we similarly evaluated neurons from healthy elderly control brains and AD brains, and provide molecular information about an earlier state during AD pathogenesis. Significant overlapping expression changes were identified in both NDAD and AD brains compared to controls and may thus define a timeline of AD pathogenesis for which factors involved in formation of AD pathologies already demonstrate expression changes in NDAD brains. Overall,we have generated a high-quality, low PMI, novel expression data set that defines the neuronal tran-scriptome in healthy elderly, NDAD, and AD brains. This resource will help to elucidate AD pathogenesis and identifies novel targets for developing improved diagnostics and therapeutics against AD. Lastly, we provide this data set to the scientific community as a public resource.

Supplementary Material

Refer to Web version on PubMed Central for supplementary material.

Acknowledgments

We would like to thank Nick Lehmans (Translational Genomics Research Institute) for help in setting up the supplementary data site, Lucia Sue (Sun Health Research Institute) for help with obtaining neuropathological data, and Elizabeth Salomon (Translational Genomics Research Institute) for assistance with GEO data posting. We would also like to thank the National Institute on Aging's Alzheimer's Disease Centers program and the National Alzheimer's Coordinating Center for help in obtaining samples for analysis.

This project was funded by grants from: the National Institute on Aging (#K01AG024079 to TD; 1-RO1-AG023193 to DAS; RO1-5U24NS051872 to DAS (NIH Neuroscience Microarray Consortium); P30 AG19610 to EMR; P50 AG05681 to JCM; P01 AG03991 to JCM; AG05128 for the Duke University ADC), the National Alzheimer's Coordinating Center (U01AG016976), the Arizona Alzheimer's Research Center (to EMR) under a collaborative agreement from the National Institute on Aging, and the State of Arizona to the Arizona Parkinson's Disease Center (Arizona Biomedical Research Commission contract 0011).

References

Angelie E, Bonmartin A, Boudraa A, Gonnaud PM, Mallet JJ, Sappey-Marinier D. Regional differences and metabolic changes in normal aging of the human brain: proton MR spectroscopic imaging study. Am. J. Neuroradiol 2001;22(1):119–127. [PubMed: 11158897]

Barrachina M, Castano E, Ferrer I. TaqMan PCR assay in the control of RNA normalization in human post-mortem brain tissue. Neu-rochem. Int 2006;49(3):276–284.

Belizaire R, Komanduri C, Wooten K, Chen M, Thaller C, Janz R. Characterization of synaptogyrin 3 as a new synaptic vesicle protein. J. Comp. Neurol 2004;470(3):266–281. [PubMed: 14755516]

Benson DL, Colman DR, Huntley GW. Molecules, maps and synapse specificity. Nat. Rev. Neurosci 2001;2(12):899–909. [PubMed: 11733797]

Blesa R, Mohr E, Miletich RS, Hildebrand K, Sampson M, Chase TN. Cerebral metabolic changes in Alzheimer's disease: neu-robehavioral patterns. Dementia 1996;7(5):239–245. [PubMed: 8872413]

Bobinski M, de Leon MJ, Convit A, De Santi S, Wegiel J, Tarshish CY, Saint Louis LA, Wisniewski HM. MRI of entorhinal cortex in mild Alzheimer's disease. Lancet 1999;353(9146):38–40. [PubMed: 10023955]

Bouras C, Hof PR, Giannakopoulos P, Michel JP, Morrison JH. Regional distribution of neurofibrillary tangles and senile plaques in the cerebral cortex of elderly patients: a quantitative evaluation of a one-year autopsy population from a geriatric hospital. Cereb. Cortex 1994;4(2):138–150. [PubMed: 8038565]

Boutajangout A, Boom A, Leroy K, Brion JP. Expression of tau mRNA and soluble tau isoforms in affected and non-affected brain areas in Alzheimer's disease. FEBS Lett 2004;576(1–2):183–189. [PubMed: 15474035]

Braak H, Braak E. The human entorhinal cortex: normal morphology and lamina-specific pathology in various diseases. Neurosci. Res 1992;15(1–2):6–31. [PubMed: 1336586]

Braak H, Braak E. Neuropathological stageing of Alzheimer-related changes. Acta Neuropathol. (Berl.) 1991;82(4):239–259. [PubMed: 1759558]

Brown NM, Torres AS, Doan PE, O'Halloran TV. Oxygen and the copper chaperone CCS regulate posttranslational activation of Cu, Zn superoxide dismutase. Proc. Natl. Acad. Sci. U.S.A 2004;101 (15):5518–5523. [PubMed: 15064408]

Conrad C, Zhu J, Conrad C, Schoenfeld D, Fang Z, Ingelsson M, Stamm S, Church G, Hyman BT. Single molecule profiling of tau gene expression in Alzheimer's disease. J. Neurochem 2007;103(3):1228–1236. [PubMed: 17727636]

Convit A, Wolf OT, de Leon MJ, Patalinjug M, Kandil E, Caraos C, Scherer A, Saint Louis LA, Cancro R. Volumetric analysis of the pre-frontal regions: findings in aging and schizophrenia. Psychiatry Res 2001;107(2):61–73. [PubMed: 11530273]

Culotta VC, Klomp LW, Strain J, Casareno RL, Krems B, Gitlin JD. The copper chaperone for superoxide dismutase. J. Biol. Chem 1997;272(38):23469–23472. [PubMed: 9295278]

Davidson Y, Gibbons L, Pritchard A, Hardicre J, Wren J, Tian J, Shi J, Stopford C, Julien C, Thompson J, Payton A, Thaker U, Hayes AJ, Iwatsubo T, Pickering-Brown SM, Pendleton N, Horan MA, Burns A, Purandare N, Lendon CL, Neary D, Snowden JS, Mann DM. Genetic associations between cathepsin D exon 2 C → T polymorphism and Alzheimer's disease, and pathological correlations with genotype. J. Neurol. Neurosurg. Psychiatry 2006;77(4):515–517. [PubMed: 16543533]

de Leon MJ, George AE, Stylopoulos LA, Smith G, Miller DC. Early marker for Alzheimer's disease: the atrophic hippocampus. Lancet 1989;2(8664):672–673. [PubMed: 2570916]

Du AT, Schuff N, Zhu XP, Jagust WJ, Miller BL, Reed BR, Kramer JH, Mungas D, Yaffe K, Chui HC, Weiner MW. Atrophy rates of entorhinal cortex in AD and normal aging. Neurology 2003;60(3): 481–486. [PubMed: 12578931]

Ferreira A, Kao HT, Feng J, Rapoport M, Greengard P. Synapsin III: developmental expression, subcellular localization, and role in axon formation. J. Neurosci 2000;20(10):3736–3744. [PubMed: 10804215]

Fox NC, Warrington EK, Stevens JM, Rossor MN. Atrophy of the hippocampal formation in early familial Alzheimer's disease. A longitudinal MRI study of at-risk members of a family with an amyloid

precursor protein 717Val-Gly mutation. Ann. N.Y. Acad. Sci 1996;777:226–232. [PubMed: 8624089]

Frisoni GB, Laakso MP, Beltramello A, Geroldi C, Bianchetti A, Soininen H, Trabucchi M. Hippocampal and entorhinal cortex atrophy in frontotemporal dementia and Alzheimer's disease. Neurology 1999;52(1):91–100. [PubMed: 9921854]

Furukawa Y, Torres AS, O'Halloran TV. Oxygen-induced maturation of SOD1: a key role for disulfide formation by the copper chaperone CCS. Embo J 2004;23(14):2872–2881. [PubMed: 15215895]

Ginsberg SD, Che S, Counts SE, Mufson EJ. Shift in the ratio of three-repeat tau and four-repeat tau mRNAs in individual cholinergic basal forebrain neurons in mild cognitive impairment and Alzheimer's disease. J. Neurochem 2006;96(5):1401–1408. [PubMed: 16478530]

Ginsberg SD, Hemby SE, Lee VM, Eberwine JH, Trojanowski JQ. Expression profile of transcripts in Alzheimer's disease tangle-bearing CA1 neurons. Ann. Neurol 2000;48(1):77–87. [PubMed: 10894219]

Goedert M, Spillantini MG, Jakes R, Rutherford D, Crowther RA. Multiple isoforms of human microtubule-associated protein tau: sequences and localization in neurofibrillary tangles of Alzheimer's disease. Neuron 1989;3(4):519–526. [PubMed: 2484340]

Hackett JT, Cochran SL, Greenfield LJ Jr, Brosius DC, Ueda T. Synapsin I injected presynaptically into goldfish mauthner axons reduces quantal synaptic transmission. J. Neurophysiol 1990;63(4):701–706. [PubMed: 2160524]

Harrison PJ, Wighton-Benn WH, Heffernan JM, Sanders MW, Pearson RC. Amyloid precursor protein mRNAs in Alzheimer's disease. Neurodegeneration 1996;5(4):409–415. [PubMed: 9117555]

Hemby SE, Trojanowski JQ, Ginsberg SD. Neuron-specific age-related decreases in dopamine receptor subtype mRNAs. J. Comp. Neurol 2003;456(2):176–183. [PubMed: 12509874]

Hilfiker S, Schweizer FE, Kao HT, Czernik AJ, Greengard P, Augustine GJ. Two sites of action for synapsin domain E in regulating neurotransmitter release. Nat. Neurosci 1998;1(1):29–35. [PubMed: 10195105]

Hyman BT, Van Hoesen GW, Damasio AR, Barnes CL. Alzheimer's disease: cell-specific pathology isolates the hippocampal formation. Science 1984;225(4667):1168–1170. [PubMed: 6474172]

Ivancevic V, Alavi A, Souder E, Mozley PD, Gur RE, Benard F, Munz DL. Regional cerebral glucose metabolism in healthy volunteers determined by fluordeoxyglucose positron emission tomography: appearance and variance in the transaxial, coronal, and sagittal planes. Clin. Nucl. Med 2000;25(8):596–602. [PubMed: 10944013]

Jack CR Jr, Petersen RC, Xu Y, O'Brien PC, Smith GE, Ivnik RJ, Tangalos EG, Kokmen E. Rate of medial temporal lobe atrophy in typical aging and Alzheimer's disease. Neurology 1998;51(4):993–999. [PubMed: 9781519]

Janz R, Sudhof TC, Hammer RE, Unni V, Siegelbaum SA, Bol-shakov VY. Essential roles in synaptic plasticity for synaptogyrin I and synaptophysin I. Neuron 1999;24(3):687–700. [PubMed: 10595519]

Johnston JA, Norgren S, Ravid R, Wasco W, Winblad B, Lannfelt L, Cowburn RF. Quantification of APP and APLP2 mRNA in APOE genotyped Alzheimer's disease brains. Brain Res. Mol. Brain Res 1996;43(1–2):85–95. [PubMed: 9037522]

Jovanovic JN, Czernik AJ, Fienberg AA, Greengard P, Sihra TS. Synapsins as mediators of BDNF-enhanced neurotransmitter release. Nat. Neurosci 2000;3(4):323–329. [PubMed: 10725920]

Jovanovic JN, Sihra TS, Nairn AC, Hemmings HC Jr, Greengard P, Czernik AJ. Opposing changes in phosphorylation of specific sites in synapsin I during Ca2+-dependent glutamate release in isolated nerve terminals. J. Neurosci 2001;21(20):7944–7953. [PubMed: 11588168]

Kitano-Takahashi M, Morita H, Kondo S, Tomizawa K, Kato R, Tanio M, Shirota Y, Takahashi H, Sugio S, Kohno T. Expression, purification and crystallization ofahuman tau-tubulin kinase 2 that phosphorylates tau protein. Acta Crystallogr. Sect. F: Struct. Biol. Cryst. Commun 2007;63(Pt 7):602–604.

Kuwano R, Miyashita A, Arai H, Asada T, Imagawa M, Shoji M, Higuchi S, Urakami K, Kakita A, Takahashi H, Tsukie T, Toyabe S, Akazawa K, Kanazawa I, Ihara Y. Dynamin-binding protein gene on chromosome 10q is associated with late-onset Alzheimer's disease. Hum. Mol. Genet 2006;15(13):2170–2182. [PubMed: 16740596]

LaFerla FM. Calcium dyshomeostasis and intracellular signalling in Alzheimer's disease. Nat. Rev. Neurosci 2002;3(11):862–872. [PubMed: 12415294]

Li L, Chin LS, Shupliakov O, Brodin L, Sihra TS, Hvalby O, Jensen V, Zheng D, McNamara JO, Greengard P, Andersen P. Impairment of synaptic vesicle clustering and of synaptic transmission, and increased seizure propensity, in synapsin I-deficient mice. Proc. Natl. Acad. Sci. U.S.A 1995;92 (20):9235–9239. [PubMed: 7568108]

Liang WS, Dunckley T, Beach TG, Grover A, Mastroeni D, Ramsey K, Caselli RJ, Kukull WA, McKeel D, Morris JC, Hulette CM, Schmechel D, Reiman EM, Rogers J, Stephan DA. Altered neuronal gene expression in brain regions differentially affected by Alzheimer's Disease: a reference data set. Physiol. Genomics. 2008

Liang WS, Dunckley T, Beach TG, Grover A, Mastroeni D, Walker DG, Caselli RJ, Kukull WA, McKeel D, Morris JC, Hulette C, Schmechel D, Alexander GE, Reiman EM, Rogers J, Stephan DA. Gene expression profiles in anatomically and functionally distinct regions of the normal aged human brain. Physiol. Genomics 2007;28(3):311–322. [PubMed: 17077275]

Livak KJ, Schmittgen TD. Analysis of relative gene expression data using real-time quantitative PCR and the 2(-Delta Delta C(T)) method. Methods 2001;25(4):402–408. [PubMed: 11846609]

Llinas R, Gruner JA, Sugimori M, McGuinness TL, Greengard P. Regulation by synapsin I and Ca(2+)-calmodulin-dependent protein kinase II of the transmitter release in squid giant synapse. J. Physiol 1991;436:257–282. [PubMed: 1676419]

Llinas R, McGuinness TL, Leonard CS, Sugimori M, Greengard P. Intraterminal injection of synapsin I or calcium/calmodulin-dependent protein kinase II alters neurotransmitter release at the squid giant synapse. Proc. Natl. Acad. Sci. U.S.A 1985;82(9):3035–3039. [PubMed: 2859595]

Loessner A, Alavi A, Lewandrowski KU, Mozley D, Souder E, Gur RE. Regional cerebral function determined by FDG-PET in healthy volunteers: normal patterns and changes with age. J. Nucl. Med 1995;36(7):1141–1149. [PubMed: 7790936]

Lohmann SM, Ueda T, Greengard P. Ontogeny of synaptic phos-phoproteins in brain. Proc. Natl. Acad. Sci. U.S.A 1978;75(8):4037–4041. [PubMed: 211513]

Lustbader JW, Cirilli M, Lin C, Xu HW, Takuma K, Wang N, Caspersen C, Chen X, Pollak S, Chaney M, Trinchese F, Liu S, Gunn-Moore F, Lue LF, Walker DG, Kuppusamy P, Zewier ZL, Arancio O, Stern D, Yan SS, Wu H. ABAD directly links Abeta to mitochondrial toxicity in Alzheimer's disease. Science 2004;304(5669):448–452. [PubMed: 15087549]

Mariani E, Seripa D, Ingegni T, Nocentini G, Mangialasche F, Ercolani S, Cherubini A, Metastasio A, Pilotto A, Senin U, Mecocci P. Interaction of CTSD and A2M polymorphisms in the risk for Alzheimer's disease. J. Neurol. Sci 2006;247(2):187–191. [PubMed: 16784755]

Markesbery WR. Oxidative stress hypothesis in Alzheimer's disease. Free Radic. Biol. Med 1997;23(1): 134–147. [PubMed: 9165306]

Matsui T, Ingelsson M, Fukumoto H, Ramasamy K, Kowa H, Frosch MP, Irizarry MC, Hyman BT. Expression of APP pathway mRNAs and proteins in Alzheimer's disease. Brain Res 2007;1161:116–123. [PubMed: 17586478]

Mattson MP, Chan SL. Neuronal and glial calcium signaling in Alzheimer's disease. Cell Calcium 2003;34(4–5):385–397. [PubMed: 12909083]

Melloni RH Jr, DeGennaro LJ. Temporal onset of synapsin I gene expression coincides with neuronal differentiation during the development of the nervous system. J. Comp. Neurol 1994;342(3):449–462. [PubMed: 8021345]

Metsaars WP, Hauw JJ, van Welsem ME, Duyckaerts C. A grading system of Alzheimer disease lesions in neocortical areas. Neurobiol. Aging 2003;24(4):563–572. [PubMed: 12714113]

Mielke R, Herholz K, Grond M, Kessler J, Heiss WD. Clinical deterioration in probable Alzheimer's disease correlates with progressive metabolic impairment of association areas. Dementia 1994;5(1): 36–41. [PubMed: 8156085]

Mielke R, Kessler J, Szelies B, Herholz K, Wienhard K, Heiss WD. Normal and pathological aging—findings of positron-emission-tomography. J. Neural. Transm 1998;105(8–9):821–837. [PubMed: 9869321]

Mirra SS, Heyman A, McKeel D, Sumi SM, Crain BJ, Brownlee LM, Vogel FS, Hughes JP, van Belle G, Berg L. The consortium to establish a registry for Alzheimer's Disease (CERAD). Part II.

Standardization of the neuropathologic assessment of Alzheimer's disease. Neurology 1991;41(4): 479–486. [PubMed: 2011243]

Moeller JR, Ishikawa T, Dhawan V, Spetsieris P, Mandel F, Alexander GE, Grady C, Pietrini P, Eidelberg D. The metabolic topography of normal aging. J. Cereb. Blood Flow Metab 1996;16(3):385–398. [PubMed: 8621743]

Nixon RA. The calpains in aging and aging-related diseases. Ageing Res. Rev 2003;2(4):407–418. [PubMed: 14522243]

Oyama F, Shimada H, Oyama R, Titani K, Ihara Y. Beta-amyloid protein precursor and tau mRNA levels versus beta-amyloid plaque and neurofibrillary tangles in the aged human brain. J. Neurochem 1993;60(5):1658–1664. [PubMed: 8473889]

Oyama F, Shimada H, Oyama R, Titani K, Ihara Y. Differential expression of beta amyloid protein precursor (APP) and tau mRNA in the aged human brain: individual variability and correlation between APP-751 and four-repeat tau. J. Neuropathol. Exp. Neurol 1991;50(5):560–578. [PubMed: 1910077]

Papassotiropoulos A, Bagli M, Kurz A, Kornhuber J, Forstl H, Maier W, Pauls J, Lautenschlager N, Heun R. A genetic variation of cathepsin D is a major risk factor for Alzheimer's disease. Ann. Neurol 2000;47(3):399–403. [PubMed: 10716266]

Preece P, Virley DJ, Costandi M, Coombes R, Moss SJ, Mudge AW, Jazin E, Cairns NJ. Amyloid precursor protein mRNA levels in Alzheimer's disease brain. Brain Res. Mol. Brain Res 2004;122 (1):1–9. [PubMed: 14992810]

Rae TD, Torres AS, Pufahl RA, O'Halloran TV. Mechanism of Cu, Zn-superoxide dismutase activation by the human metallochaperone hCCS. J. Biol. Chem 2001;276(7):5166–5176. [PubMed: 11018045]

Reich M, Ohm K, Angelo M, Tamayo P, Mesirov JP. GeneClus-ter 2.0: an advanced toolset for bioarray analysis. Bioinformatics 2004;20(11):1797–1798. [PubMed: 14988123]

Robinson CA, Clark AW, Parhad IM, Fung TS, Bou SS. Gene expression in Alzheimer neocortex as a function of age and pathologic severity. Neurobiol. Aging 1994;15(6):681–690. [PubMed: 7891822]

Rosahl TW, Spillane D, Missler M, Herz J, Selig DK, Wolff JR, Hammer RE, Malenka RC, Sudhof TC. Essential functions of synapsins I and II in synaptic vesicle regulation. Nature 1995;375(6531):488–493. [PubMed: 7777057]

Rothstein JD, Dykes-Hoberg M, Corson LB, Becker M, Cleveland DW, Price DL, Culotta VC, Wong PC. The copper chaperone CCS is abundant in neurons and astrocytes in human and rodent brain. J. Neurochem 1999;72(1):422–429. [PubMed: 9886096]

Saraswati S, Adolfsen B, Littleton JT. Characterization of the role of the Synaptotagmin family as calcium sensors in facilitation and asynchronous neurotransmitter release. Proc. Natl. Acad. Sci. U.S.A 2007;104(35):14122–14127. [PubMed: 17709738]

Scheiffele P. Cell-cell signaling during synapse formation in the CNS. Annu. Rev. Neurosci 2003;26:485–508. [PubMed: 12626697]

Schmidt PJ, Rae TD, Pufahl RA, Hamma T, Strain J, O'Halloran TV, Culotta VC. Multiple protein domains contribute to the action of the copper chaperone for superoxide dismutase. J. Biol. Chem 1999;274(34):23719–23725. [PubMed: 10446130]

Selkoe DJ. Alzheimer's disease: genes, proteins, and therapy. Physiol. Rev 2001;81(2):741–766. [PubMed: 11274343]

Selkoe DJ, Schenk D. Alzheimer's disease: molecular understanding predicts amyloid-based therapeutics. Annu. Rev. Pharmacol. Toxicol 2003;43:545–584. [PubMed: 12415125]

Sinha S, Anderson JP, Barbour R, Basi GS, Caccavello R, Davis D, Doan M, Dovey HF, Frigon N, Hong J, Jacobson-Croak K, Jewett N, Keim P, Knops J, Lieberburg I, Power M, Tan H, Tatsuno G, Tung J, Schenk D, Seubert P, Suomensaari SM, Wang S, Walker D, Zhao J, McConlogue L, John V. Purification and cloning of amyloid precursor protein beta-secretase from human brain. Nature 1999;402(6761):537–540. [PubMed: 10591214]

Small GW, Ercoli LM, Silverman DH, Huang SC, Komo S, Bookheimer SY, Lavretsky H, Miller K, Siddarth P, Rasgon NL, Mazziotta JC, Saxena S, Wu HM, Mega MS, Cummings JL, Saunders AM, Pericak-Vance MA, Roses AD, Barrio JR, Phelps ME. Cerebral metabolic and cognitive decline in persons at genetic risk for Alzheimer's disease. Proc. Natl. Acad. Sci. U.S.A 2000;97(11):6037–6042. [PubMed: 10811879]

Sollner T, Whiteheart SW, Brunner M, Erdjument-Bromage H, Geromanos S, Tempst P, Rothman JE. SNAP receptors implicated in vesicle targeting and fusion. Nature 1993;362(6418):318–324. [PubMed: 8455717]

Sugita S, Janz R, Sudhof TC. Synaptogyrins regulate Ca2+-dependent exocytosis in PC12 cells. J. Biol. Chem 1999;274(27):18893–18901. [PubMed: 10383386]

Thal DR, Rub U, Orantes M, Braak H. Phases of A beta-deposition in the human brain and its relevance for the development of AD. Neurology 2002;58(12):1791–1800. [PubMed: 12084879]

Vanderklish PW, Bahr BA. The pathogenic activation of calpain: a marker and mediator of cellular toxicity and disease states. Int. J. Exp. Pathol 2000;81(5):323–339. [PubMed: 11168679]

Vassar R, Bennett BD, Babu-Khan S, Kahn S, Mendiaz EA, Denis P, Teplow DB, Ross S, Amarante P, Loeloff R, Luo Y, Fisher S, Fuller J, Edenson S, Lile J, Jarosinski MA, Biere AL, Curran E, Burgess T, Louis JC, Collins F, Treanor J, Rogers G, Citron M. Beta-secretase cleavage of Alzheimer's amyloid precursor protein by the transmembrane aspartic protease BACE. Science 1999;286(5440): 735–741. [PubMed: 10531052]

Waites CL, Craig AM, Garner CC. Mechanisms of vertebrate synaptogenesis. Annu. Rev. Neurosci 2005;28:251–274. [PubMed: 16022596]

Yan R, Bienkowski MJ, Shuck ME, Miao H, Tory MC, Pauley AM, Brashier JR, Stratman NC, Mathews WR, Buhl AE, Carter DB, Tomasselli AG, Parodi LA, Heinrikson RL, Gurney ME. Membrane-anchored aspartyl protease with Alzheimer's disease beta-secretase activity. Nature 1999;402(6761): 533–537. [PubMed: 10591213]

Yan SD, Fu J, Soto C, Chen X, Zhu H, Al-Mohanna F, Collison K, Zhu A, Stern E, Saido T, Tohyama M, Ogawa S, Roher A, Stern D. An intracellular protein that binds amyloid-beta peptide and mediates neurotoxicity in Alzheimer's disease. Nature 1997;389(6652):689–695. [PubMed: 9338779]

Zhou W, Scott SA, Shelton SB, Crutcher KA. Cathepsin D-mediated proteolysis of apolipoprotein E: possible role in Alzheimer's disease. Neuroscience 2006;143(3):689–701. [PubMed: 16997486]

entorhinal cortex

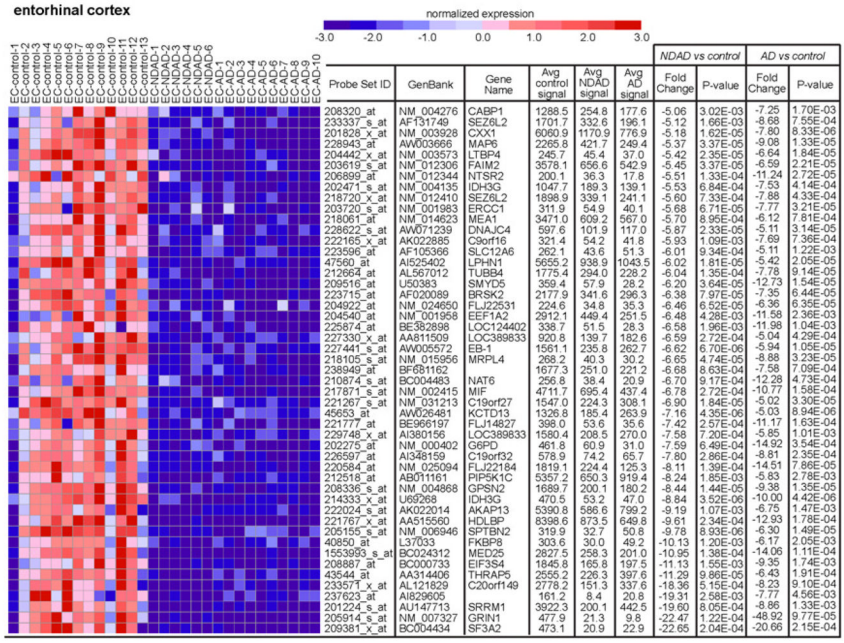

Probe Set ID	GenBank	Gene Name	Avg control signal	Avg NDAD signal	Avg AD signal	NDAD vs control Fold Change	NDAD vs control P-value	AD vs control Fold Change	AD vs control P-value
208320_at	NM_004276	CABP1	1288.5	254.8	177.6	-5.06	3.02E-03	-7.25	1.70E-03
233337_s_at	AF131749	SEZ6L2	1701.7	332.6	196.1	-5.12	1.66E-03	-8.68	7.55E-04
201828_x_at	NM_003928	CPX1	6060.9	1170.9	776.9	-5.18	1.62E-05	-7.80	8.33E-06
228943_at	AW003666	MAP6	2265.8	421.7	249.4	-5.37	3.37E-05	-9.08	1.33E-05
204442_x_at	NM_003573	LTBP4	245.7	45.4	37.0	-5.42	2.35E-05	-6.64	1.84E-05
203619_s_at	NM_012306	FAIM2	3578.1	656.6	542.9	-5.45	3.37E-05	-6.59	2.21E-05
206899_at	NM_012344	NTSR2	200.1	36.3	17.8	-5.51	1.33E-04	-11.24	2.72E-05
202471_s_at	NM_004135	IDH3G	1047.7	189.3	139.1	-5.53	6.84E-04	-7.53	4.14E-04
218720_x_at	NM_012410	SEZ6L2	1898.9	339.1	241.1	-5.60	7.33E-04	-7.88	4.33E-04
203720_s_at	NM_001983	ERCC1	311.9	54.9	40.1	-5.68	6.71E-05	-7.77	3.21E-05
218061_at	NM_014623	MEA1	3471.0	609.2	567.0	-5.70	8.95E-04	-6.12	7.81E-04
228622_s_at	AW071239	DNAJC4	597.6	101.9	117.0	-5.87	2.33E-05	-5.11	3.14E-05
222165_x_at	AK022885	C9orf16	321.4	54.2	41.8	-5.93	1.09E-03	-7.69	7.36E-04
223596_at	AF105366	SLC12A6	262.1	43.6	51.3	-6.01	9.34E-04	-5.11	1.22E-03
47560_at	AI525402	LPHN1	5655.2	938.9	1043.5	-6.02	1.81E-05	-5.42	2.05E-05
212864_at	AL567012	TUBB4	1775.4	294.0	228.2	-6.04	1.35E-04	-7.78	9.14E-05
209516_at	U50383	SMYD5	359.4	57.9	28.2	-6.20	3.64E-05	-12.73	1.54E-05
223715_at	AF020089	BRSK2	2177.9	341.6	296.3	-6.38	7.97E-05	-7.35	6.44E-05
204922_at	NM_024650	FLJ22531	224.6	34.8	35.3	-6.46	6.52E-05	-6.36	6.35E-05
204540_at	NM_001958	EEF1A2	2912.1	449.4	251.5	-6.48	4.28E-03	-11.58	2.36E-03
225674_at	BE382898	LOC124402	338.7	51.5	28.3	-6.58	1.96E-03	-11.98	1.04E-03
227330_x_at	AA811509	LOC389833	920.8	139.7	182.6	-6.59	2.72E-04	-5.04	4.29E-04
227441_s_at	AW005572	EB-1	1561.1	235.8	262.7	-6.62	6.70E-06	-5.94	1.05E-05
218105_s_at	NM_015956	MRPL4	268.2	40.3	30.2	-6.65	4.74E-05	-8.88	3.23E-05
238949_at	BF681162		1677.3	251.0	221.2	-6.68	8.63E-04	-7.58	7.09E-04
210874_s_at	BC004483	NAT6	256.8	38.4	20.9	-6.70	9.17E-04	-12.28	4.73E-04
217871_s_at	NM_002415	MIF	4711.7	695.4	437.4	-6.78	2.72E-04	-10.77	1.58E-04
221267_s_at	NM_031213	C19orf27	1547.0	224.3	308.1	-6.90	1.84E-05	-5.02	3.30E-05
45653_at	AW026481	KCTD13	1326.8	185.4	263.9	-7.16	4.35E-06	-5.03	8.94E-06
221777_at	BE966197	FLJ14827	398.0	53.6	35.6	-7.42	2.57E-04	-11.17	1.63E-04
229748_x_at	AI380156	LOC389833	1580.4	208.5	270.0	-7.58	7.20E-04	-5.85	1.01E-03
202275_at	NM_000402	G6PD	461.8	60.9	31.0	-7.59	6.49E-04	-14.92	3.54E-04
226597_at	AI348159	C19orf32	578.9	74.2	65.7	-7.80	2.86E-04	-8.81	2.35E-04
220584_at	NM_025094	FLJ22184	1819.1	224.4	125.3	-8.11	1.39E-04	-14.51	7.86E-05
212518_at	AB011161	PIP5K1C	5357.2	650.3	919.4	-8.24	1.85E-03	-5.83	2.78E-03
208336_s_at	NM_004868	GPSN2	1689.7	200.1	180.2	-8.44	1.44E-05	-9.38	1.35E-05
214333_x_at	U69268	IDH3G	470.5	53.2	47.0	-8.84	3.52E-06	-10.00	4.42E-06
222024_s_at	AK022014	AKAP13	5390.8	586.6	799.2	-9.19	1.07E-03	-6.75	1.47E-03
221767_x_at	AA515560	HDLBP	8398.6	873.5	649.8	-9.61	2.34E-04	-12.93	1.78E-04
205155_s_at	NM_006946	SPTBN2	319.9	32.7	50.8	-9.78	8.93E-06	-6.30	1.49E-05
40850_at	L37033	FKBP8	303.6	30.0	49.2	-10.13	1.20E-03	-6.17	2.05E-03
1553993_s_at	BC024312	MED25	2827.5	258.3	201.0	-10.95	1.38E-04	-14.06	1.11E-04
208887_at	BC000733	EIF3S4	1845.8	165.8	197.5	-11.13	1.55E-03	-9.35	1.74E-03
43544_at	AA314406	THRAP5	2555.2	226.3	397.6	-11.29	9.86E-05	-6.43	1.91E-04
233571_x_at	AL121829	C20orf149	2778.2	151.3	337.6	-18.36	5.15E-04	-8.23	9.10E-04
237623_at	AI829605		161.2	8.4	20.8	-19.31	2.58E-03	-7.77	4.56E-03
201224_s_at	AU147713	SRRM1	3922.3	200.1	442.5	-19.60	8.05E-04	-8.86	1.33E-03
205914_s_at	NM_007327	GRIN1	477.9	21.3	9.8	-22.47	1.22E-04	-48.92	9.77E-05
209381_x_at	BC004434	SF3A2	473.1	20.9	22.9	-22.65	2.04E-04	-20.66	2.15E-04

hippocampus

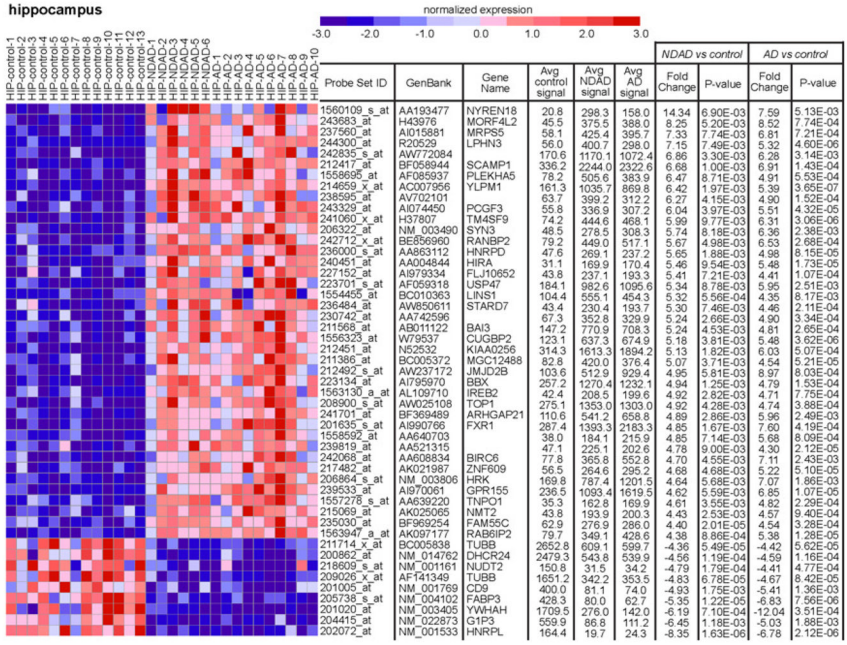

Probe Set ID	GenBank	Gene Name	Avg control signal	Avg NDAD signal	Avg AD signal	NDAD vs control Fold Change	NDAD vs control P-value	AD vs control Fold Change	AD vs control P-value
1560109_s_at	AA193477	NYREN18	20.8	298.3	158.0	14.34	6.90E-03	7.59	5.13E-03
243683_at	H43976	MORF4L2	45.5	375.5	388.0	8.25	5.20E-03	8.52	7.74E-04
237560_at	AI015881	MRPS5	58.1	425.4	395.7	7.33	7.74E-03	6.81	7.21E-04
244300_at	R20529	LPHN3	56.0	400.7	298.0	7.15	7.49E-03	5.32	4.60E-06
242835_s_at	AW772084		170.6	1170.1	1072.4	6.86	3.30E-03	6.28	3.14E-03
212417_at	BF058944	SCAMP1	336.2	2244.0	2132.6	6.68	1.10E-03	6.91	1.43E-04
1558695_at	AF085937	PLEKHA5	78.2	505.6	383.9	6.47	8.71E-03	4.91	5.53E-04
214659_x_at	AC007956	YLPM1	161.3	1035.7	869.8	6.42	1.97E-03	5.39	3.65E-07
238595_at	AV702101		63.7	399.2	312.2	6.27	4.15E-03	4.90	1.52E-04
243329_at	AI074450	PCGF3	55.8	336.9	307.2	6.04	3.97E-03	5.51	4.32E-05
241060_x_at	H37807	TM4SF9	74.2	444.6	468.1	5.99	9.77E-03	6.31	3.06E-06
206322_at	NM_003490	SYN3	48.5	278.5	308.3	5.74	8.18E-03	6.36	2.38E-03
242712_x_at	BE856960	RANBP2	79.2	449.0	517.1	5.67	4.98E-03	6.53	2.68E-04
236000_x_at	AA863112	HNRPD	47.6	269.1	237.2	5.65	1.88E-03	4.98	8.15E-05
240451_at	AA004844	HIRA	31.1	169.9	170.4	5.46	9.54E-03	5.48	1.73E-05
227152_at	AI979334	FLJ10652	43.8	237.1	193.3	5.41	7.21E-03	4.41	1.07E-04
223701_s_at	AF059318	USP47	184.1	982.6	1095.6	5.34	8.78E-03	5.95	2.51E-03
1554455_at	BC010363	LIN51	104.4	555.1	454.3	5.32	5.56E-04	4.35	8.17E-03
236484_at	AW850611	STARD7	43.4	230.4	193.7	5.30	7.46E-03	4.46	2.11E-04
230742_at	AA742596		67.3	352.8	329.9	5.24	2.66E-03	4.90	3.34E-04
211568_at	AB011122	BAI3	147.2	770.9	708.3	5.24	4.53E-03	4.81	2.65E-04
1556323_at	W79537	CUGBP2	123.1	637.3	674.9	5.18	3.81E-03	5.48	3.62E-06
212451_at	N52532	KIAA0256	314.3	1613.3	1894.2	5.13	1.82E-03	6.03	5.07E-04
211386_at	BC005372	MGC12488	82.8	420.0	376.4	5.07	3.71E-03	4.54	5.21E-05
212492_s_at	AW237172	JMJD2B	103.6	512.9	929.4	4.95	5.81E-03	8.97	8.03E-04
223134_at	AI795970	BBX	257.2	1270.4	1232.1	4.94	1.25E-03	4.79	1.53E-04
1563130_a_at	AL109710	IREB2	42.4	208.5	199.6	4.92	2.82E-03	4.71	7.75E-04
208900_s_at	AW025108	TOP1	275.1	1353.0	1303.0	4.92	4.28E-03	4.74	3.88E-04
241701_at	BF369489	ARHGAP21	110.6	541.2	658.8	4.89	2.86E-03	5.96	2.49E-03
201635_s_at	AI990766	FXR1	287.4	1393.3	2183.3	4.85	1.67E-03	7.60	4.19E-04
1558592_at	AA640703		38.0	184.1	215.9	4.85	7.14E-03	5.68	8.09E-04
239819_at	AA521315		47.1	225.1	202.6	4.78	9.00E-03	4.30	2.12E-05
242068_at	AA608834	BIRC6	77.8	365.8	552.8	4.70	4.55E-03	7.11	2.43E-03
217482_at	AK021987	ZNF609	56.5	264.6	295.2	4.68	4.68E-03	5.22	5.10E-05
206864_s_at	NM_003806	HRK	169.8	787.4	1201.5	4.64	5.68E-03	7.07	1.86E-03
239533_at	AI970061	GPR155	236.5	1093.4	1619.5	4.62	5.59E-03	6.85	1.07E-05
1557278_s_at	AA639220	TNPO1	35.3	162.8	169.9	4.61	3.55E-03	4.82	2.29E-04
215069_at	AK025065	NMT2	43.8	193.9	200.3	4.43	2.53E-03	4.57	9.40E-04
235030_at	BF969254	FAM55C	62.9	276.9	286.0	4.40	2.01E-05	4.54	3.28E-04
1563947_a_at	AK097177	RAB8IP2	79.7	349.1	428.6	4.38	8.86E-04	5.38	1.28E-05
211714_x_at	BC005838	TUBB	2652.8	609.1	599.7	-4.36	5.49E-05	-4.42	5.62E-05
200862_at	NM_014762	DHCR24	2479.3	543.8	539.9	-4.56	1.19E-04	-4.59	1.16E-04
218609_s_at	NM_001161	NUDT2	150.8	31.5	34.2	-4.79	1.79E-04	-4.41	4.77E-04
209026_x_at	AF141349	TUBB	1651.2	342.2	353.5	-4.83	6.78E-05	-4.67	8.42E-05
201005_at	NM_001769	CD9	400.0	81.1	74.0	-4.93	1.75E-03	-5.41	1.36E-03
205738_s_at	NM_004102	FABP3	428.3	80.0	62.7	-5.35	1.22E-05	-6.83	7.56E-06
201020_at	NM_003405	YWHAH	1709.5	276.0	142.0	-6.19	7.10E-04	-12.04	3.51E-04
204415_at	NM_022873	G1P3	559.9	86.8	111.2	-6.45	1.18E-03	-5.03	1.88E-03
202072_at	NM_001533	HNRPL	164.4	19.7	24.3	-8.35	1.63E-06	-6.78	2.12E-06

middle temporal gyrus

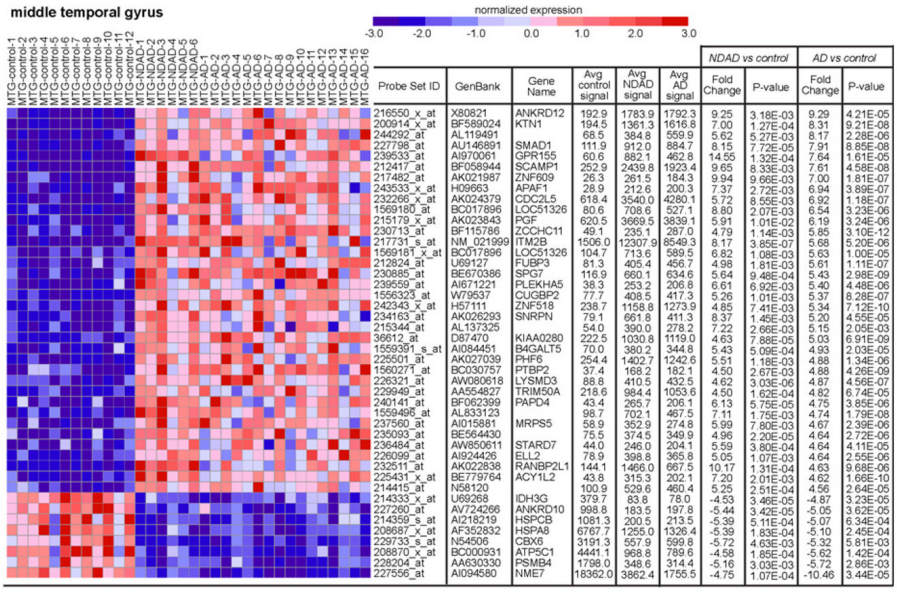

Probe Set ID	GenBank	Gene Name	Avg control signal	Avg NDAD signal	Avg AD signal	NDAD vs control Fold Change	NDAD vs control P-value	AD vs control Fold Change	AD vs control P-value
216550_x_at	X80821	ANKRD12	192.9	1783.9	1792.3	9.25	3.18E-03	9.29	4.21E-05
200914_x_at	BF589024	KTN1	194.5	1361.3	1616.8	7.00	1.27E-04	8.31	9.21E-08
244292_at	AL119491		68.5	384.8	559.9	5.62	5.27E-03	8.17	2.28E-06
227798_at	AU146891	SMAD1	111.9	912.0	884.7	8.15	7.72E-05	7.91	8.85E-08
239533_at	AI970061	GPR155	60.6	882.1	462.8	14.55	1.32E-04	7.64	1.61E-05
212417_at	BF058944	SCAMP1	252.9	2439.8	1923.4	9.65	8.33E-03	7.61	4.58E-08
217482_at	AK021987	ZNF609	26.3	251.5	184.3	9.94	9.66E-03	7.00	1.81E-07
243533_x_at	H09663	APAF1	28.9	212.6	200.3	7.37	2.72E-03	6.94	3.89E-07
232266_x_at	AK024379	CDC2L5	618.4	3540.0	4280.1	5.72	8.55E-03	6.92	1.18E-07
1569180_at	BC017896	LOC51326	80.6	708.6	527.1	8.80	2.07E-03	6.54	3.23E-06
215179_x_at	AK023843	PGF	620.5	3669.5	3839.1	5.91	1.01E-02	6.19	3.24E-06
230713_at	BF115786	ZCCHC11	49.1	235.1	287.0	4.79	1.14E-03	5.85	3.10E-12
217731_s_at	NM_021999	ITM2B	1506.0	12307.9	8549.3	8.17	3.85E-07	5.68	5.20E-06
1569181_x_at	BC017896	LOC51326	104.7	713.6	589.5	6.82	1.08E-03	5.63	1.00E-05
212824_at	U89127	FUBP3	81.3	405.4	456.7	4.98	1.81E-03	5.61	1.11E-07
230885_at	BE670386	SPG7	116.9	660.1	634.6	5.64	9.48E-04	5.43	2.98E-09
239559_at	AI671221	PLEKHA5	38.3	253.2	206.8	6.61	6.92E-03	5.40	4.48E-06
1556323_at	W79537	CUGBP2	77.7	408.5	417.3	5.26	1.01E-03	5.37	8.28E-07
242343_x_at	H57111	ZNF518	238.7	1158.8	1273.9	4.85	7.41E-03	5.34	7.12E-10
234163_at	AK026293	SNRPN	79.1	661.8	411.3	8.37	1.45E-03	5.20	4.55E-05
215344_at	AL137325		54.0	390.0	278.2	7.22	2.66E-03	5.15	2.05E-03
36612_at	D87470	KIAA0280	222.5	1030.8	1119.0	4.63	7.88E-05	5.03	6.91E-09
1559351_s_at	AI084451	B4GALT5	70.0	380.2	344.8	5.43	5.09E-04	4.93	2.03E-05
225501_at	AK027039	PHF6	254.4	1402.7	1242.6	5.51	1.18E-03	4.88	1.34E-06
1560271_at	BC030757	PTBP2	37.4	168.2	182.1	4.50	2.67E-03	4.88	4.26E-09
226321_at	AW080618	LYSMD3	88.8	410.5	432.5	4.62	3.03E-06	4.87	4.56E-07
229949_at	AA554827	TRIM50A	218.6	984.4	1053.6	4.50	1.62E-04	4.82	6.74E-05
240141_at	BF062399	PAPD4	43.4	265.7	206.1	6.13	5.75E-05	4.75	3.85E-06
1559496_at	AL833123		98.7	702.1	467.5	7.11	1.75E-03	4.74	1.79E-08
237560_at	AI015881	MRPS5	58.9	352.9	274.8	5.99	7.80E-03	4.67	2.39E-06
235093_at	BE564430		75.5	374.5	349.9	4.96	2.20E-05	4.64	2.72E-06
236484_at	AW850611	STARD7	44.0	246.0	204.1	5.59	3.80E-04	4.64	4.11E-05
226099_at	AI924426	ELL2	78.9	398.8	365.8	5.05	1.07E-03	4.64	2.55E-06
232511_at	AK022838	RANBP2L1	144.1	1466.0	667.5	10.17	1.31E-04	4.63	9.68E-06
225431_x_at	BE779764	ACY1L2	43.8	315.3	202.1	7.20	2.01E-03	4.62	1.66E-10
214415_at	N58120		100.9	529.6	460.4	5.25	2.51E-04	4.56	2.64E-05
214333_x_at	U69268	IDH3G	379.7	83.8	78.0	-4.53	3.46E-05	-4.87	3.23E-05
227260_at	AV724266	ANKRD10	998.8	183.5	197.8	-5.44	3.42E-05	-5.05	3.62E-05
214359_s_at	AI218219	HSPCB	1081.3	200.5	213.5	-5.39	5.11E-04	-5.07	6.34E-04
208687_x_at	AF352832	HSPA8	6767.7	1255.0	1326.4	-5.39	1.83E-04	-5.10	2.45E-04
229733_s_at	N54506	CBX6	3191.3	557.9	599.8	-5.72	4.63E-03	-5.32	5.81E-03
208870_x_at	BC000931	ATP5C1	4441.1	968.8	789.6	-4.58	1.85E-04	-5.62	1.42E-04
228204_at	AA630330	PSMB4	1798.0	348.6	314.4	-5.16	3.03E-03	-5.72	2.86E-03
227556_at	AI094580	NME7	16362.0	3862.4	1755.5	-4.75	1.07E-04	-10.46	3.44E-05

posterior cingulate cortex

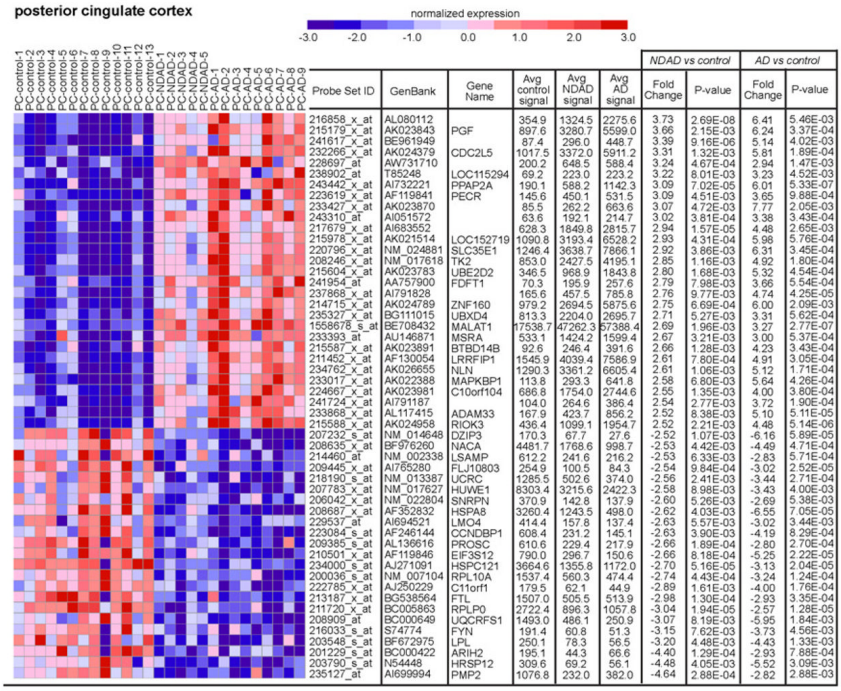

Probe Set ID	GenBank	Gene Name	Avg control signal	Avg NDAD signal	Avg AD signal	NDAD vs control Fold Change	NDAD vs control P-value	AD vs control Fold Change	AD vs control P-value
216858_x_at	AL080112		354.9	1324.5	2275.6	3.73	2.69E-08	6.41	5.46E-03
215179_x_at	AK023843	PGF	897.6	3280.7	5599.0	3.66	2.15E-03	6.24	3.37E-04
241617_x_at	BE961949		87.4	296.0	448.7	3.39	9.16E-06	5.14	4.02E-03
232266_x_at	AK024379	CDC2L5	1017.5	3372.0	5911.2	3.31	1.32E-03	5.81	1.89E-04
228697_at	AW731710		200.2	648.5	588.4	3.24	4.67E-04	2.94	1.47E-03
238902_at	T85248	LOC115294	69.2	223.0	223.2	3.22	8.01E-03	3.23	4.52E-03
243442_x_at	AI732221	PPAP2A	190.1	588.2	1142.3	3.09	1.02E-05	6.01	5.33E-07
223619_x_at	AF119841	PECR	145.6	450.1	531.5	3.09	4.51E-03	3.65	9.88E-04
233427_at	AK023870		85.5	262.2	663.6	3.07	4.72E-03	7.77	2.05E-03
243310_at	AI051572		63.6	192.1	214.7	3.02	3.81E-04	3.38	3.43E-04
217679_x_at	AI683552		628.3	1849.8	2815.7	2.94	1.57E-05	4.48	2.65E-03
215978_x_at	AK021514	LOC152719	1090.8	3193.4	6528.2	2.93	4.31E-04	5.98	5.76E-04
220796_x_at	NM_024881	SLC35E1	1246.4	3638.7	7866.1	2.92	3.86E-03	6.31	3.45E-04
208246_x_at	NM_017618	TK2	853.0	2427.5	4195.1	2.85	1.16E-03	4.92	1.80E-04
215604_x_at	AK023783	UBE2D2	346.5	968.9	1843.8	2.80	1.68E-03	5.32	4.54E-04
241954_at	AA757900	FDFT1	70.3	195.9	257.6	2.79	7.98E-03	3.66	5.54E-04
237868_x_at	AI791828		165.6	457.5	785.8	2.76	9.77E-03	4.74	4.25E-05
214715_x_at	AK024789	ZNF160	979.2	2694.5	5875.6	2.75	6.69E-04	6.00	2.09E-03
235327_x_at	BG111015	UBXD4	813.3	2204.0	2695.7	2.71	5.27E-03	3.31	5.62E-04
1558678_s_at	BE708432	MALAT1	16338.7	47262.3	57388.4	2.69	1.96E-03	3.27	2.77E-07
233393_at	AU146871	MSRA	533.1	1424.2	1599.4	2.67	3.21E-03	3.00	5.37E-04
215587_x_at	AK023891	BTBD14B	92.6	246.4	391.6	2.66	1.28E-03	4.23	3.43E-04
211452_x_at	AF130054	LRRFIP1	1545.9	4039.4	7586.9	2.61	7.80E-04	4.91	3.05E-04
234762_x_at	AK026655	NLN	1290.3	3361.2	6605.4	2.61	1.06E-03	5.12	1.71E-04
233017_x_at	AK022388	MAPKBP1	113.8	293.3	641.8	2.58	6.80E-03	5.64	4.26E-04
224667_x_at	AK023981	C10orf104	686.8	1754.0	2744.6	2.55	1.35E-03	4.00	3.80E-04
241724_x_at	AI791187		104.0	264.6	386.4	2.54	2.77E-03	3.72	1.90E-04
233868_x_at	AL117415	ADAM33	167.9	423.7	856.2	2.52	8.38E-03	5.10	5.11E-05
215586_x_at	AK024958	RIOK3	436.4	1099.1	1954.7	2.52	2.21E-03	4.48	5.14E-06
207232_s_at	NM_014648	DZIP3	170.3	67.7	27.6	-2.52	1.07E-03	-6.16	5.89E-05
208635_x_at	BF976260	NACA	4481.7	1768.6	998.7	-2.53	4.42E-03	-4.49	4.71E-04
214460_at	NM_002338	LSAMP	612.2	241.6	216.2	-2.53	6.33E-03	-2.83	5.71E-04
209445_x_at	AI765280	FLJ10803	254.9	100.5	84.3	-2.54	9.84E-04	-3.02	2.52E-05
218190_s_at	NM_013387	UCRC	1285.5	502.6	374.0	-2.56	2.41E-03	-3.44	2.71E-04
207783_x_at	NM_017627	HUWE1	8303.4	3215.6	2422.3	-2.58	8.98E-03	-3.43	4.00E-03
206042_x_at	NM_022804	SNRPN	370.9	142.8	137.9	-2.60	5.26E-03	-2.69	5.38E-03
208687_x_at	AF352832	HSPA8	3260.4	1243.5	498.0	-2.62	4.03E-03	-6.55	7.05E-05
229537_at	AI694521	LMO4	414.4	157.8	137.4	-2.63	5.57E-03	-3.02	3.44E-03
223084_s_at	AF246144	CCNDBP1	608.4	231.2	145.1	-2.63	3.90E-03	-4.19	8.29E-04
209385_s_at	AL136616	PROSC	610.6	229.4	217.9	-2.66	1.89E-04	-2.80	2.70E-04
210501_x_at	AF119846	EIF3S12	790.0	296.7	150.6	-2.66	8.18E-04	-5.25	2.22E-05
204000_s_at	AJ271091	HSPC121	3664.6	1355.8	1172.0	-2.70	5.16E-05	-3.13	2.04E-05
200036_s_at	NM_007104	RPL10A	1537.4	560.3	474.4	-2.74	4.43E-04	-3.24	1.24E-04
222785_x_at	AJ250229	C11orf1	179.5	62.1	44.9	-2.89	1.61E-03	-4.00	1.76E-04
213187_x_at	BG538564	FTL	1507.0	505.5	513.9	-2.98	1.30E-04	-2.93	3.35E-04
211720_x_at	BC005863	RPLP0	2722.4	896.3	1057.8	-3.04	1.94E-05	-2.57	1.28E-05
208909_at	BC000649	UQCRFS1	1493.0	486.1	250.9	-3.07	8.19E-03	-5.95	1.84E-03
216033_s_at	S74774	FYN	191.4	60.8	51.3	-3.15	7.62E-03	-3.73	4.56E-03
203548_s_at	BF672975	LPL	250.1	78.3	56.5	-3.20	4.48E-03	-4.43	1.33E-03
201229_s_at	BC000422	ARIH2	195.1	44.3	66.6	-4.40	1.29E-04	-2.93	7.88E-04
203790_s_at	N54448	HRSP12	309.6	69.2	56.1	-4.48	4.05E-03	-5.52	3.09E-03
235127_at	AI699994	PMP2	1076.8	232.0	382.0	-4.64	2.88E-04	-2.82	2.88E-03

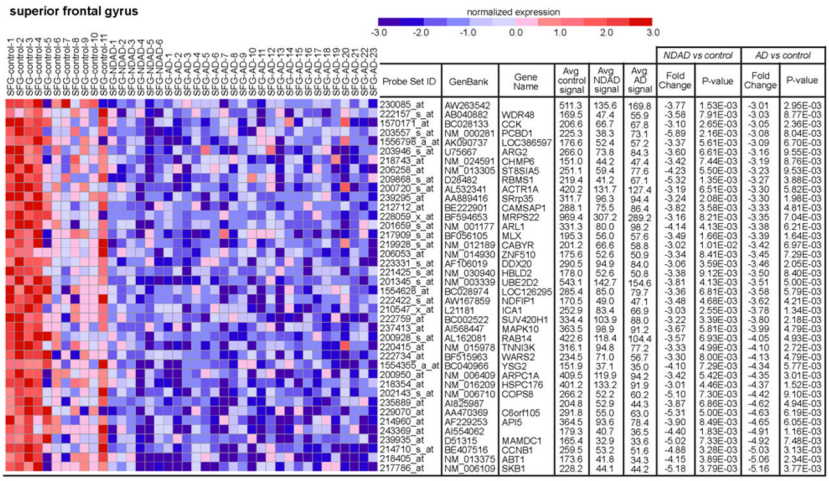

Probe Set ID	GenBank	Gene Name	Avg control signal	Avg NDAD signal	Avg AD signal	NDAD vs control Fold Change	NDAD vs control P-value	AD vs control Fold Change	AD vs control P-value
230085_at	AW263542		511.3	135.6	169.8	-3.77	1.53E-03	-3.01	2.95E-03
222157_s_at	AB040882	WDR48	169.5	47.4	56.9	-3.58	7.91E-03	-3.03	8.77E-03
1570177_at	BC028133	CCK	206.6	66.7	67.8	-3.10	2.65E-03	-3.05	2.36E-03
203557_s_at	NM_000281	PCBD1	225.3	38.3	73.1	-5.89	2.16E-03	-3.08	8.04E-03
1556798_a_at	AK090737	LOC386597	176.6	52.4	57.2	-3.37	5.61E-03	-3.09	6.70E-03
203946_s_at	U75667	ARG2	266.0	73.8	84.3	-3.60	6.61E-03	-3.16	9.55E-03
218743_at	NM_024591	CHMP6	151.0	44.2	47.4	-3.42	7.44E-03	-3.19	8.76E-03
206258_at	NM_013305	ST8SIA5	251.1	59.4	77.6	-4.23	5.50E-03	-3.23	9.53E-03
209868_s_at	D28482	RBMS1	219.4	41.2	67.1	-5.32	1.35E-03	-3.27	3.88E-03
200720_s_at	AL532341	ACTR1A	420.2	131.7	127.4	-3.19	6.51E-03	-3.30	5.82E-03
238295_at	AA889416	SRrp35	311.7	96.3	94.4	-3.24	2.08E-03	-3.30	1.98E-03
212712_at	BE222901	CAMSAP1	288.1	75.5	86.4	-3.82	3.58E-03	-3.33	4.81E-03
228059_x_at	BF594653	MRPS22	969.4	307.2	289.2	-3.16	8.21E-03	-3.35	7.04E-03
201659_s_at	NM_001177	ARL1	331.3	80.0	98.2	-4.14	4.13E-03	-3.38	6.21E-03
217909_s_at	BF056105	MLX	195.3	56.0	57.6	-3.49	1.66E-03	-3.39	1.64E-03
219928_s_at	NM_012189	CABYR	201.2	66.6	58.8	-3.02	1.01E-02	-3.42	6.97E-03
206053_at	NM_014930	ZNF510	175.6	52.6	50.9	-3.34	8.41E-03	-3.45	7.29E-03
223331_s_at	AF106019	DDX20	290.5	94.9	84.0	-3.06	3.59E-03	-3.46	2.05E-03
221425_s_at	NM_030940	HBLD2	178.0	52.6	50.8	-3.38	9.12E-03	-3.50	8.40E-03
201345_s_at	NM_003339	UBE2D2	543.1	142.7	154.6	-3.81	4.13E-03	-3.51	5.00E-03
1554628_at	BC028974	LOC126295	285.4	85.0	79.7	-3.36	6.81E-03	-3.58	5.79E-03
222422_s_at	AW167859	NDFIP1	170.5	49.0	47.1	-3.48	4.68E-03	-3.62	4.21E-03
210547_x_at	L21181	ICA1	252.9	83.4	66.9	-3.03	2.55E-03	-3.78	1.34E-03
222759_at	BC002522	SUV420H1	334.4	103.9	88.0	-3.22	3.39E-03	-3.80	2.18E-03
237413_at	AI568447	MAPK10	363.5	98.9	91.2	-3.67	5.81E-03	-3.99	4.79E-03
200928_s_at	AL162081	RAB14	422.6	118.4	104.4	-3.57	6.93E-03	-4.05	4.93E-03
220415_at	NM_015978	TNNI3K	316.1	94.8	77.2	-3.33	4.99E-03	-4.10	2.72E-03
222734_at	BF515963	WARS2	234.5	71.0	56.7	-3.30	8.00E-03	-4.13	4.79E-03
1554355_a_at	BC040966	YSG2	151.9	37.1	35.0	-4.10	7.29E-03	-4.34	5.77E-03
200950_at	NM_006409	ARPC1A	409.5	119.9	94.2	-3.42	5.42E-03	-4.35	3.01E-03
218354_at	NM_016209	HSPC176	401.2	133.2	91.9	-3.01	4.46E-03	-4.37	1.52E-03
202143_s_at	NM_006710	COPS8	266.2	52.2	60.2	-5.10	7.30E-03	-4.42	9.10E-03
235889_at	AI825987		204.8	52.9	44.3	-3.87	6.86E-03	-4.62	4.94E-03
229070_at	AA470369	C6orf105	291.8	55.0	63.0	-5.31	5.00E-03	-4.63	6.19E-03
214960_at	AF229253	API5	364.5	93.6	78.4	-3.90	8.49E-03	-4.65	6.05E-03
243369_at	AI554062		179.3	40.7	36.5	-4.40	1.83E-03	-4.91	1.16E-03
239935_at	D61315	MAMDC1	165.4	32.9	33.6	-5.02	7.33E-03	-4.92	7.48E-03
214710_s_at	BE407516	CCNB1	259.5	53.2	51.6	-4.88	3.28E-03	-5.03	3.13E-03
218405_at	NM_013375	ABT1	173.6	41.8	34.3	-4.15	3.89E-03	-5.06	2.34E-03
217786_at	NM_006109	SKB1	228.2	44.1	44.2	-5.18	3.79E-03	-5.16	3.77E-03

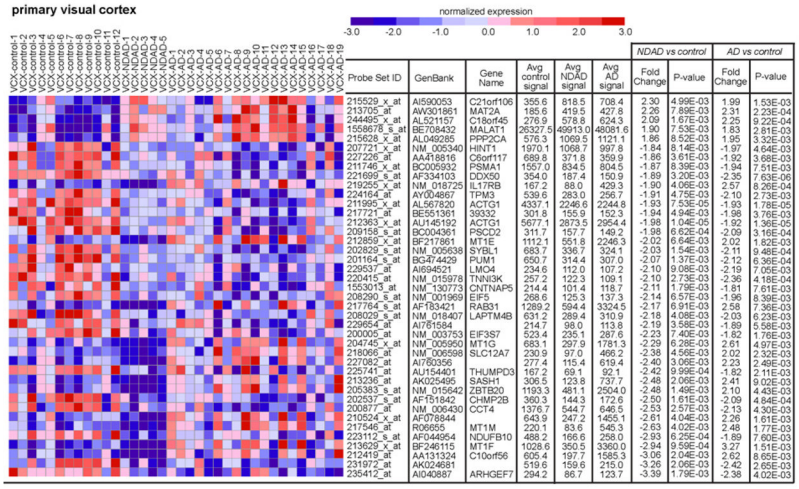

Probe Set ID	GenBank	Gene Name	Avg control signal	Avg NDAD signal	Avg AD signal	NDAD vs control Fold Change	NDAD vs control P-value	AD vs control Fold Change	AD vs control P-value
215529_x_at	AI590053	C21orf106	355.6	818.5	708.4	2.30	4.99E-03	1.99	1.53E-03
213705_at	AW301861	MAT2A	185.6	419.5	427.8	2.26	7.89E-03	2.31	2.23E-04
244465_x_at	AL521157	C18orf45	276.9	578.8	624.3	2.09	1.67E-03	2.25	9.22E-04
1558678_s_at	BE708432	MALAT1	26327.5	49913.0	48081.6	1.90	7.53E-03	1.83	2.81E-03
215628_x_at	AL049285	PPP2CA	576.3	1069.5	1121.1	1.86	8.52E-03	1.95	3.32E-03
207721_x_at	NM_005340	HINT1	1970.1	1068.7	997.8	-1.84	8.14E-03	-1.97	4.64E-03
227226_at	AA418616	C6orf117	689.8	371.8	359.9	-1.86	3.61E-03	-1.92	3.68E-03
211746_x_at	BC005932	PSMA1	1557.0	834.5	804.5	-1.87	8.39E-03	-1.94	7.51E-03
221689_s_at	AF334103	DDX50	354.0	187.4	150.9	-1.89	3.20E-03	-2.35	7.63E-06
219255_x_at	NM_018725	IL17RB	167.2	88.0	429.3	-1.90	4.06E-03	2.57	8.26E-04
224164_at	AY004867	TPM3	539.6	283.0	256.7	-1.91	4.75E-03	-2.10	2.73E-03
211995_x_at	AL567820	ACTG1	4337.1	2246.6	2244.8	-1.93	7.53E-05	-1.93	1.78E-05
217721_at	BE551361	39332	301.8	155.9	152.3	-1.94	4.94E-03	-1.98	3.76E-03
212363_x_at	AU145192	ACTG1	5677.1	2873.5	2954.4	-1.98	1.04E-05	-1.92	1.36E-05
209158_s_at	BC004361	PSCD2	311.7	157.7	149.2	-1.98	8.62E-04	-2.09	3.16E-04
212859_x_at	BF217861	MT1E	1112.1	551.8	2246.3	-2.02	6.64E-03	2.02	1.82E-03
202829_s_at	NM_005638	SYBL1	683.7	336.7	324.1	-2.03	1.54E-03	-2.11	9.48E-04
201164_s_at	BG774429	PUM1	650.7	314.4	307.0	-2.07	1.37E-03	-2.12	8.36E-04
229537_at	AI694521	LMO4	234.6	112.0	107.2	-2.10	9.08E-03	-2.19	7.05E-03
220415_at	NM_015978	TNNI3K	257.2	122.3	109.1	-2.10	2.73E-03	-2.36	4.18E-04
1553013_at	NM_130773	GRINA4P5	214.4	101.4	118.7	-2.11	1.79E-03	-1.81	7.61E-03
208290_s_at	NM_001969	EIF5	268.6	125.3	137.3	-2.14	6.57E-03	-1.96	8.39E-03
217764_s_at	AF183421	RAB31	1289.2	594.4	3324.5	-2.17	6.91E-03	2.58	7.36E-03
208029_s_at	NM_018407	LAPTM4B	631.2	289.4	310.9	-2.18	4.08E-03	-2.03	6.23E-03
229654_at	AI781584		214.7	98.0	113.8	-2.19	3.58E-03	-1.89	5.58E-03
200005_at	NM_003753	EIF3S7	523.4	235.1	287.6	-2.23	7.40E-03	-1.82	1.76E-03
204745_x_at	NM_005950	MT1G	683.1	297.9	1781.3	-2.29	6.26E-03	2.61	4.97E-03
218066_at	NM_006598	SLC12A7	230.9	97.0	466.2	-2.38	4.56E-03	2.02	2.32E-03
227082_at	AI780356		277.4	115.4	619.4	-2.40	3.06E-03	2.23	2.49E-03
225741_at	AU154401	THUMPD3	167.2	69.1	92.1	-2.42	9.95E-04	1.82	2.11E-03
213236_at	AK025495	SASH1	306.5	123.8	737.7	-2.48	2.06E-03	2.41	9.02E-03
205383_s_at	NM_015642	ZBTB20	1193.3	481.1	2504.0	-2.48	1.49E-03	2.10	4.43E-03
202537_s_at	AF151842	CHMP2B	360.3	144.3	172.6	-2.50	1.61E-03	-2.09	4.84E-04
200877_at	NM_006430	CCT4	1376.7	544.7	646.5	-2.53	2.57E-03	-2.13	4.30E-03
210524_x_at	AF078844		643.9	247.2	1455.1	-2.61	4.04E-03	2.26	1.61E-03
217546_at	R06655	MT1M	220.1	83.6	546.3	-2.63	4.02E-03	2.48	1.77E-03
223112_s_at	AF044954	NDUFB10	488.2	166.6	258.0	-2.93	6.25E-04	-1.89	7.60E-03
213629_x_at	BF246115	MT1F	1028.6	350.5	3360.0	-2.94	9.59E-04	3.27	1.51E-03
212419_at	AA131324	C10orf56	605.4	197.7	1585.3	-3.06	2.04E-03	2.62	8.65E-03
231972_at	AK024681		519.6	159.6	215.0	-3.26	2.06E-03	-2.42	2.65E-03
235412_at	AI040887	ARHGEF7	294.2	86.7	123.7	-3.39	1.79E-03	-2.38	4.02E-03

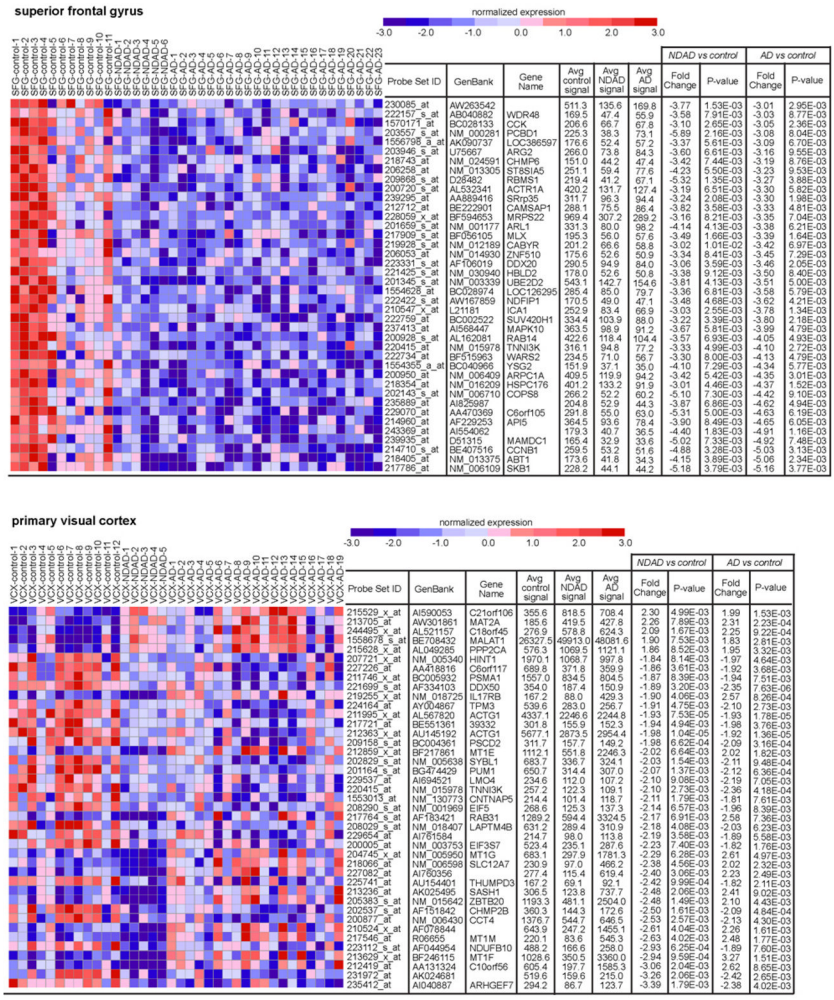

Probe Set ID	GenBank	Gene Name	Avg control signal	Avg NDAD signal	Avg AD signal	NDAD vs control Fold Change	NDAD vs control P-value	AD vs control Fold Change	AD vs control P-value
230085_at	AW263542		511.3	135.6	169.8	-3.77	1.53E-03	-3.01	2.95E-03
222157_s_at	AB040882	WDR48	169.5	47.4	56.9	-3.58	7.91E-03	-3.03	8.77E-03
1570177_at	BC028133	CCK	206.6	66.7	67.8	-3.10	2.65E-03	-3.05	2.36E-03
203557_s_at	NM_000281	PCBD1	225.3	38.3	73.1	-5.89	2.16E-03	-3.08	8.04E-03
1556798_a_at	AK090737	LOC386597	176.6	52.4	57.2	-3.37	5.61E-03	-3.09	6.70E-03
203946_s_at	U75667	ARG2	266.0	73.8	84.3	-3.60	6.61E-03	-3.16	9.55E-03
218743_at	NM_024591	CHMP6	151.0	44.2	47.4	-3.42	7.44E-03	-3.19	8.76E-03
206258_at	NM_013305	ST8SIA5	251.1	59.4	77.6	-4.23	5.50E-03	-3.23	9.53E-03
209868_s_at	D28482	RBMS1	219.4	41.2	67.1	-5.32	1.35E-03	-3.27	3.88E-03
200720_s_at	AL532341	ACTR1A	420.2	131.7	127.4	-3.19	6.51E-03	-3.30	5.82E-03
238295_at	AA889416	SRrp35	311.7	96.3	94.4	-3.24	2.08E-03	-3.30	1.98E-03
212712_at	BE222901	CAMSAP1	288.1	75.5	86.4	-3.82	3.58E-03	-3.33	4.81E-03
228059_x_at	BF594653	MRPS22	969.4	307.2	289.2	-3.16	8.21E-03	-3.35	7.04E-03
201659_s_at	NM_001177	ARL1	331.3	80.0	98.2	-4.14	4.13E-03	-3.38	6.21E-03
217909_s_at	BF056105	MLX	195.3	56.0	57.6	-3.49	1.66E-03	-3.39	1.64E-03
219928_s_at	NM_012189	CABYR	201.2	66.6	58.8	-3.02	1.01E-02	-3.42	6.97E-03
206053_at	NM_014930	ZNF510	175.6	52.6	50.9	-3.34	8.41E-03	-3.45	7.29E-03
223331_s_at	AF106019	DDX20	290.5	94.9	84.0	-3.06	3.59E-03	-3.46	2.05E-03
221425_s_at	NM_030940	HBLD2	178.0	52.6	50.8	-3.38	9.12E-03	-3.50	8.40E-03
201345_s_at	NM_003339	UBE2D2	543.1	142.7	154.6	-3.81	4.13E-03	-3.51	5.00E-03
1554628_at	BC028974	LOC126295	285.4	85.0	79.7	-3.36	6.81E-03	-3.58	5.79E-03
222422_s_at	AW167859	NDFIP1	170.5	49.0	47.1	-3.48	4.68E-03	-3.62	4.21E-03
210547_x_at	L21181	ICA1	252.9	83.4	66.9	-3.03	2.55E-03	-3.78	1.34E-03
222759_at	BC002522	SUV420H1	334.4	103.9	88.0	-3.22	3.39E-03	-3.80	2.18E-03
237413_at	AI568447	MAPK10	363.5	98.9	91.2	-3.67	5.81E-03	-3.99	4.79E-03
200928_s_at	AL162081	RAB14	422.6	118.4	104.4	-3.57	6.93E-03	-4.05	4.93E-03
220415_at	NM_015978	TNNI3K	316.1	94.8	77.2	-3.33	4.99E-03	-4.10	2.72E-03
222734_at	BF515963	WARS2	234.5	71.0	56.7	-3.30	8.00E-03	-4.13	4.79E-03
1554355_a_at	BC040966	YSG2	151.9	37.1	35.0	-4.10	7.29E-03	-4.34	5.77E-03
200950_at	NM_006409	ARPC1A	409.5	119.9	94.2	-3.42	5.42E-03	-4.35	3.01E-03
218354_at	NM_016209	HSPC176	401.2	133.2	91.9	-3.01	4.46E-03	-4.37	1.52E-03
202143_s_at	NM_006710	COPS8	266.2	52.2	60.2	-5.10	7.30E-03	-4.42	9.10E-03
235889_at	AI829987		204.8	52.9	44.3	-3.87	6.86E-03	-4.62	4.94E-03
229070_at	AA470369	C6orf105	291.8	55.0	63.0	-5.31	5.00E-03	-4.63	6.19E-03
214960_at	AF229253	API5	364.5	93.6	78.4	-3.90	8.49E-03	-4.65	6.05E-03
243369_at	AI554062		179.3	40.7	36.5	-4.40	1.83E-03	-4.91	1.16E-03
239935_at	D61315	MAMDC1	165.4	32.9	33.6	-5.02	7.33E-03	-4.92	7.48E-03
214710_s_at	BE407516	CCNB1	259.5	53.2	51.6	-4.88	3.28E-03	-5.03	3.13E-03
218405_at	NM_013375	ABT1	173.6	41.8	34.3	-4.15	3.89E-03	-5.06	2.34E-03
217786_at	NM_006109	SKB1	228.2	44.1	44.2	-5.18	3.79E-03	-5.16	3.77E-03

Probe Set ID	GenBank	Gene Name	Avg control signal	Avg NDAD signal	Avg AD signal	NDAD vs control Fold Change	NDAD vs control P-value	AD vs control Fold Change	AD vs control P-value
215529_x_at	AI590053	C21orf106	355.6	818.5	708.4	2.30	4.99E-03	1.99	1.53E-03
213705_at	AW301861	MAT2A	185.6	419.5	427.8	2.26	7.89E-03	2.31	2.23E-04
244465_x_at	AL521157	C19orf45	276.9	578.8	624.3	2.09	1.67E-03	2.25	9.22E-04
1558678_s_at	BE708432	MALAT1	26327.5	49913.0	48081.6	1.90	7.53E-03	1.83	2.81E-03
215628_x_at	AL049285	PPP2CA	576.3	1069.5	1121.1	1.86	8.52E-03	1.95	3.32E-03
207721_x_at	NM_005340	HINT1	1970.1	1068.7	997.8	-1.84	8.14E-03	-1.97	4.64E-03
227226_at	AA418816	C6orf117	689.8	371.8	359.9	-1.86	3.61E-03	-1.92	3.68E-03
211746_x_at	BC005932	PSMA1	1557.0	834.5	804.5	-1.87	8.39E-03	-1.94	7.51E-03
221689_s_at	AF334103	DDX50	354.0	187.4	150.9	-1.89	3.20E-03	-2.35	7.63E-06
219255_x_at	NM_018725	IL17RB	167.2	88.0	429.3	-1.90	4.06E-03	2.57	8.26E-04
224164_at	AY004867	TPM3	539.6	283.0	256.7	-1.91	4.75E-03	-2.10	2.73E-03
211995_x_at	AL567820	ACTG1	4337.1	2246.6	2244.8	-1.93	7.53E-05	-1.93	1.78E-05
217721_at	BE551361	39332	301.8	155.9	152.3	-1.94	4.94E-03	-1.98	3.76E-03
212363_x_at	AU145192	ACTG1	5677.1	2873.5	2954.4	-1.98	1.04E-05	-1.92	1.36E-05
209158_s_at	BC004361	PSCD2	311.7	157.7	149.2	-1.98	8.62E-04	-2.09	3.16E-04
212859_x_at	BF217861	MT1E	1112.1	551.8	2246.3	-2.02	6.64E-03	2.02	1.82E-03
202829_s_at	NM_005638	SYBL1	683.7	336.7	324.1	-2.03	1.54E-03	-2.11	9.48E-04
201164_s_at	BG774429	PUM1	650.7	314.4	307.0	-2.07	1.37E-03	-2.12	8.36E-04
229537_at	AI694521	LMO4	234.6	112.0	107.2	-2.10	9.08E-03	-2.19	7.05E-03
220415_at	NM_015978	TNNI3K	257.2	122.3	109.1	-2.10	2.73E-03	-2.36	4.18E-04
1553013_at	NM_130773	ANTNAP5	214.4	101.4	118.7	-2.11	1.79E-03	-1.81	7.61E-03
208290_s_at	NM_001969	EIF5	268.6	125.3	137.3	-2.14	6.57E-03	-1.96	8.39E-03
217764_s_at	AF183421	RAB31	1289.2	594.4	3324.5	-2.17	6.91E-03	2.58	7.36E-03
208029_s_at	NM_018407	LAPTM4B	631.2	289.4	310.9	-2.18	4.08E-03	-2.03	6.23E-03
229654_at	AI781584		214.7	98.0	113.8	-2.19	3.58E-03	-1.89	5.58E-03
200005_at	NM_003753	EIF3S7	523.4	235.1	287.6	-2.23	7.40E-03	-1.82	1.76E-03
204745_x_at	NM_005950	MT1G	683.1	297.9	1781.3	-2.29	6.28E-03	2.61	4.97E-03
218066_at	NM_006598	SLC12A7	230.9	97.0	466.2	-2.38	4.56E-03	2.02	2.32E-03
227082_at	AI780356		277.4	115.4	619.4	-2.40	3.06E-03	2.23	2.49E-03
225741_at	AU154401	THUMPD3	167.2	69.1	92.1	-2.42	9.95E-04	1.82	2.11E-03
213236_at	AK025495	SASH1	306.5	123.8	737.7	-2.48	2.06E-03	2.41	9.02E-03
205383_s_at	NM_015642	ZBTB20	1193.3	481.1	2504.0	-2.48	1.49E-03	2.10	4.43E-03
202537_s_at	AF151842	CHMP2B	360.3	144.3	172.6	-2.50	1.61E-03	-2.09	4.84E-04
200877_at	NM_006430	CCT4	1376.7	544.7	646.5	-2.53	2.57E-03	-2.13	4.30E-03
210524_x_at	AF078844		643.9	247.2	1455.1	-2.61	4.04E-03	2.26	1.61E-03
217546_at	R06655	MT1M	220.1	83.6	546.3	-2.63	4.02E-03	2.48	1.77E-03
223112_s_at	AF044954	NDUFB10	488.2	166.6	258.0	-2.93	6.25E-04	-1.89	7.60E-03
213629_x_at	BF246115	MT1F	1028.6	350.5	3360.0	-2.94	9.59E-04	3.27	1.51E-03
212419_at	AA131324	C10orf56	605.4	197.7	1585.3	-3.06	2.04E-03	2.62	8.65E-03
231972_at	AK024681		519.6	159.6	215.0	-3.26	2.06E-03	-2.42	2.65E-03
235412_at	AI040887	ARHGEF7	294.2	86.7	123.7	-3.39	1.79E-03	-2.38	4.02E-03

Fig. 1.

Common expression changes in NDAD and AD. Regional dendrograms of statistically significant genes ($P < 0.01$, corrected for multiple testing) demonstrating parallel expression changes are shown. Genes shown have the greatest changes in expression for both the NDAD vs. controls analysis and AD vs. controls analysis.

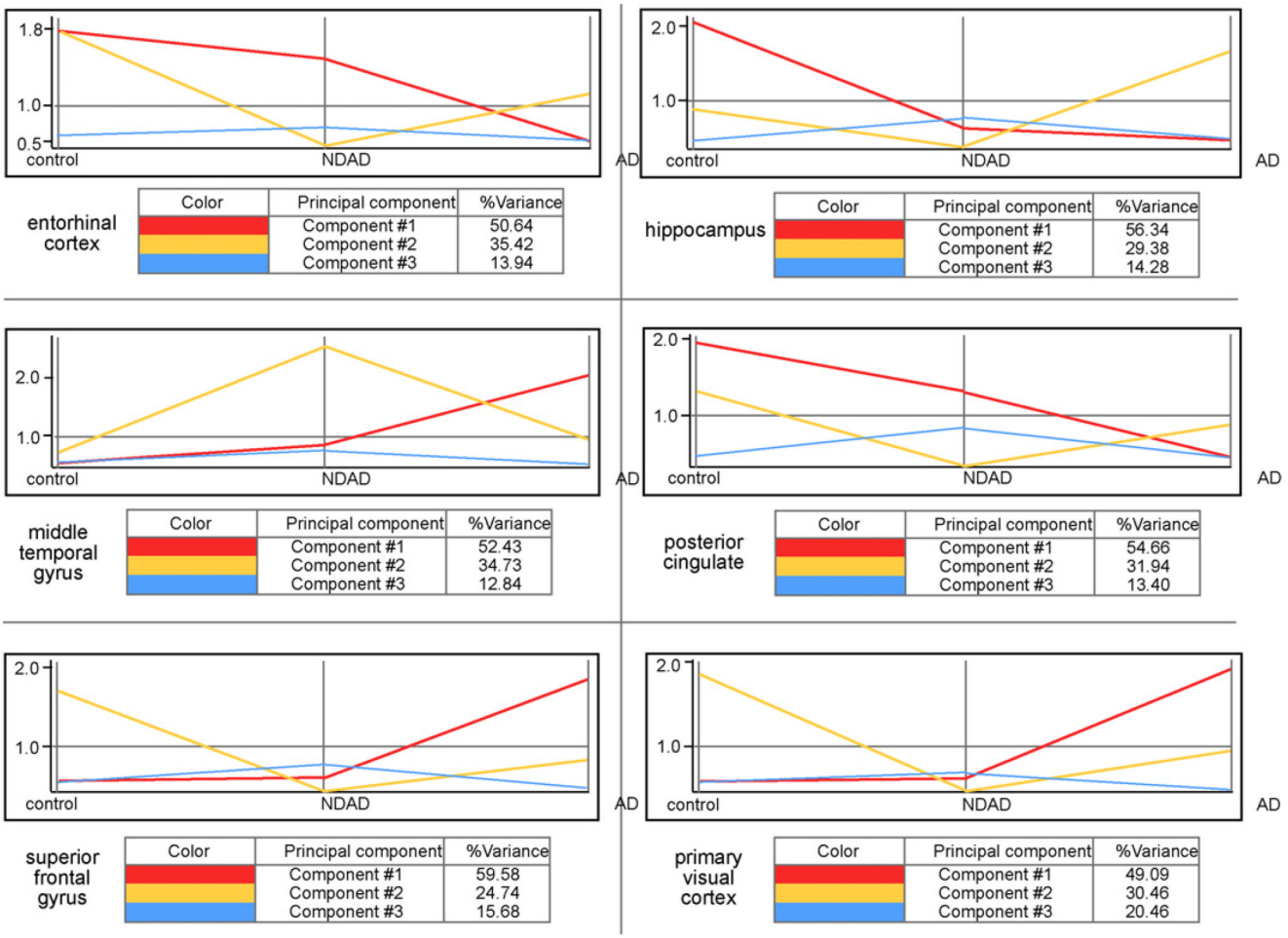

Fig. 2.

Regional principal components analysis. Three principal components are shown for each region across healthy controls, NDAD brains, and AD brains (*x*-axis). The *y*-axis represents the logged normalized intensity value. The percentage of expression variance (across controls, NDAD, and AD brains) that each component accounts for is listed.

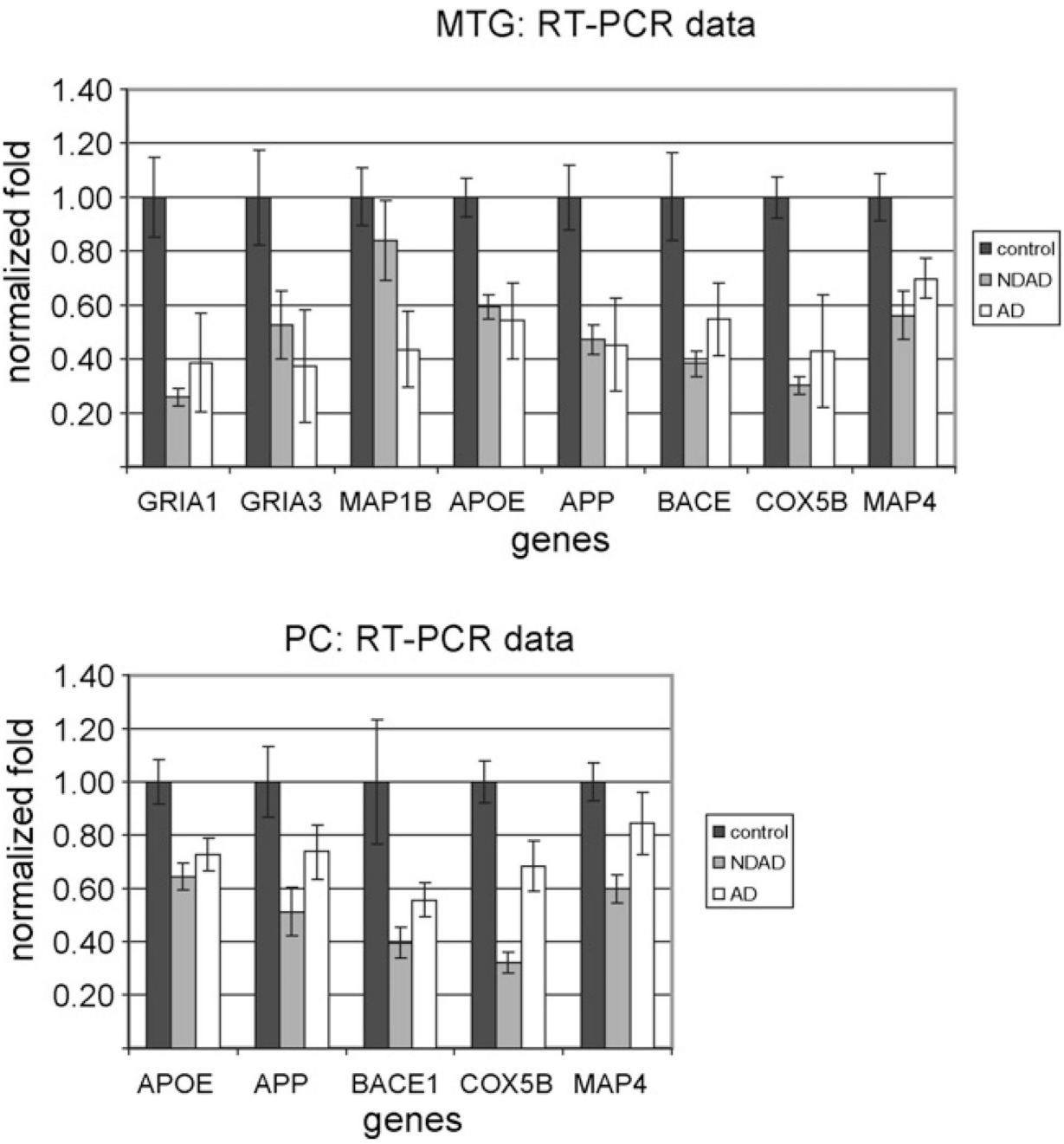

Fig. 3.

RT-PCR validation of selected genes. RT-PCR validation of expression changes identified from array analysis was performed on unprofiled MTG (controls: $n = 9$, NDAD: $n = 8$, AD: $n = 9$) and PC (controls: $n = 8$, NDAD: $n = 8$, AD: $n = 11$) samples. RT-PCR data, along with respective array data, are shown (quantitative data is listed in Table 6). Fold values normalized to controls are shown on the *y*-axis and genes are listed on the *x*-axis.

Table 1

Sample group information

	Control	NDAD	AD
Mean age	79.8 ± 9.1	86.6 ± 5.3	79.9 ± 6.9
Gender	M: 10; F: 4	M: 6; F: 4	M: 15; F: 18
EC (*n*)	13	6	10
HIP (*n*)	13	6	10
MTG (*n*)	12	6	16
PC (*n*)	13	5	9
SFG (*n*)	11	6	23
VCX (*n*)	12	5	19

Sample sizes for each sample group and brain region are shown (*n*).

Table 2

Common expression changes in NDAD and AD brains: tangle and plaque pathway factors

Probe set ID	Genbank ID	Gene symbol	Brain region	NDAD vs. control		AD vs. control	
				Fold	*P*-value*	Fold	*P*-value*
203929_s_at	AI056359	MAPT	EC	−2.32	2.41E−05	−1.46	6.76E−03
206401_s_at	J03778	MAPT	HIP	2.73	7.86E−03	1.85	1.71E−02
203928_ x_at	AI870749	MAPT	HIP	2.48	5.15E−04	2.23	6.84E−04
225379_at	AA199717	MAPT	HIP	−2.40	6.12E−05	−2.15	1.35E−04
203930_s_at	NM 016835	MAPT	MTG	−1.90	2.90E−02	−1.99	1.81E−02
225379_at	AA199717	MAPT	MTG	−2.00	7.44E−03	−2.21	3.29E−03
226653_at	AB040910	MARK1	MTG	2.51	2.76E−03	1.49	8.36E−03
239166_at	R98192	MARK3	EC	−3.75	1.47E−03	−1.10	3.90E+00
202568_s_at	AI745639	MARK3	HIP	−2.08	2.24E−05	−2.37	5.33E−06
202568_s_at	AI745639	MARK3	MTG	−1.61	2.76E−03	−1.59	8.89E−04
55065_at	AL120554	MARK4	EC	−4.32	1.51E−05	−2.39	2.44E−04
221560_at	AB049127	MARK4	EC	−5.07	1.44E−05	−2.52	2.56E−04
204247_s_at	NM 004935	CDK5	EC	−2.49	1.21E−03	−3.87	6.51E−06
204247_s_at	NM 004935	CDK5	HIP	−2.03	2.43E−03	−1.91	4.62E−03
204247_s_at	NM 004935	CDK5	MTG	−2.49	2.95E−03	−4.33	3.62E−04
209018_s_at	BF432478	PINK1	EC	−2.28	6.85E−05	−1.89	3.60E−04
209019_s_at	AF316873	PINK1	HIP	−2.61	5.56E−04	−2.23	6.52E−04
213922_at	AW294686	TTBK2	MTG	4.66	8.02E−05	3.53	3.09E−06
213922_at	AW294686	TTBK2	HIP	3.81	3.38E−04	3.52	1.17E−07
231086_at	BF939127	BACE1	EC	−1.98	4.40E−04	−1.04	6.53E+00
222463_s_at	AF190725	BACE1	EC	−3.28	1.70E−04	−1.66	1.49E−02
222462_s_at	AI653425	BACE1	EC	−3.06	1.94E−05	−1.77	1.36E−03
222462_s_at	AI653425	BACE1	HIP	−1.47	6.26E−03	−1.17	4.84E−01
217904_s_at	NM 012104	BACE1	HIP	−1.68	4.45E−03	−1.93	3.77E−05
217904_s_at	NM 012104	BACE1	MTG	−1.75	9.56E−06	−1.32	2.58E−03
203460_s_at	NM 007318	PSEN1	HIP	−1.92	5.33E−03	−1.64	3.44E−02
226577_at	N49844	PSEN1	MTG	−2.06	3.95E−03	−1.53	1.91E−02

Probe set ID	Genbank ID	Gene symbol	Brain region	NDAD vs. control		AD vs. control	
				Fold	*P*-value*	Fold	*P*-value*
203460_s_at	NM 007318	PSEN1	PC	−1.80	5.42E−03	−2.30	4.05E−04
211373_s_at	U34349	PSEN2	MTG	−1.50	4.88E−03	−1.89	4.25E−05
200602_at	NM 000484	APP	HIP	1.89	2.13E−04	2.14	3.55E−03
214953_s_at	X06989	APP	MTG	2.37	1.35E−03	1.12	1.44E+00
200602_at	NM 000484	APP	MTG	5.11	6.71E−04	3.09	8.20E−07
211277_x_at	BC004369	APP	PC	1.69	4.54E−04	3.01	2.05E−04
200602_at	NM 000484	APP	PC	2.11	1.87E−04	1.93	8.38E−04

*Corrected *P* values are shown.

Table 3

Common expression changes in NDAD and AD brains: synaptic factors

Probe set ID	Genbank ID	Gene symbol	Brain region	NDAD vs. control		AD vs. control	
				Fold	*P*-value*	Fold	*P*-value*
1556629_a_at	AI806346	SNAP25	EC	−3.26	1.46E−06	−2.52	7.50E−06
1556629_a_at	AI806346	SNAP25	HIP	2.15	6.30E−03	2.15	8.46E−05
202507_s_at	L19760	SNAP25	MTG	−4.07	1.02E−03	−14.27	2.04E−04
202508_s_at	NM 003081	SNAP25	VCX	1.90	7.75E−04	−1.28	3.33E−01
204729_s_at	NM 004603	STX1A	HIP	−1.60	5.85E−03	−1.72	5.18E−03
204729_s_at	NM 004603	STX1A	MTG	−1.69	5.35E−03	−2.45	9.18E−05
209238_at	BE966922	STX3A	HIP	−1.54	3.66E−03	−1.76	1.62E−03
230691_at	R85929	STX1B2	EC	−4.95	4.85E−07	−3.49	1.49E−06
212799_at	BE217875	STX6	MTG	1.60	6.86E−03	1.02	1.83E+01
204690_at	NM 004853	STX8	MTG	−3.06	4.38E−04	−3.10	4.36E−04
204690_at	NM 004853	STX8	HIP	−2.12	6.93E−04	−2.99	1.59E−05
212625_at	NM 003765	STX10	EC	−2.24	1.90E−04	1.09	2.15E+00
212625_at	NM 003765	STX10	MTG	−2.09	4.99E−04	−1.33	1.11E−01
221499_s_at	AK026970	STX16	VCX	−1.79	1.01E−02	1.04	6.87E+00
222708_s_at	AW014619	STX17	VCX	−2.20	8.86E−03	−1.55	1.47E−03
228091_at	AI800609	STX17	HIP	1.50	3.34E−03	1.21	3.74E−01
228091_at	AI800609	STX17	MTG	1.61	2.03E−03	1.20	4.33E−01
222708_s_at	AW014619	STX17	PC	−2.45	1.74E−04	−1.40	1.61E−01
222708_s_at	AW014619	STX17	SFG	−3.11	3.94E−03	−2.30	1.14E−02
218763_at	NM 016930	STX18	HIP	−2.18	2.51E−05	−2.34	2.20E−05
218763_at	NM 016930	STX18	MTG	−2.65	2.02E−05	−1.67	1.99E−04
218763_at	NM 016930	STX18	PC	−1.46	8.63E−03	−1.23	9.62E−01
221914_at	H19843	SYN1	EC	−7.49	1.85E−05	−4.92	4.04E−05
210247_at	AW139618	SYN2	EC	−3.11	2.34E−04	−3.31	1.79E−04
206322_at	NM 003490	SYN3	EC	−2.52	7.56E−05	−3.35	4.12E−06
221914_at	H19843	SYN1	HIP	−2.12	2.71E−04	−1.40	7.55E−02
221914_at	H19843	SYN1	MTG	−1.63	8.53E−03	−2.48	1.41E−04

Probe set ID	Genbank ID	Gene symbol	Brain region	NDAD vs. control		AD vs. control	
				Fold	*P*-value*	Fold	*P*-value*
221914_at	H19843	SYN1	PC	−1.77	3.77E−03	−1.35	2.55E−01
229039_at	BE220333	SYN2	HIP	−2.01	5.17E−03	−3.09	1.59E−04
210315_at	AF077737	SYN2	HIP	1.84	4.85E−03	1.80	1.10E−02
206322_at	NM 003490	SYN3	HIP	5.74	8.18E−03	6.36	2.38E−03
206322_at	NM 003490	SYN3	MTG	3.37	5.28E−03	2.04	7.24E−02
204287_at	NM 004711	SYNGR1	EC	−1.95	2.95E−04	−2.65	2.16E−05
205691_at	NM 004209	SYNGR3	EC	−2.37	2.06E−03	−4.73	1.15E−04
203999_at	AV731490	SYT1	MTG	−1.54	2.47E−03	−3.93	9.17E−10
223901_at	AL136594	SYT3	EC	−2.04	8.15E−04	−2.40	1.50E−04
223901_at	AL136594	SYT3	MTG	−2.01	3.08E−03	−1.94	2.47E−03
206162_x_at	NM 003180	SYT5	EC	−3.42	9.06E−05	−2.70	2.80E−04
244227_at	AI863338	SYT6	EC	−2.83	1.47E−03	1.75	6.87E−02
244227_at	AI863338	SYT6	SFG	−2.49	2.84E−03	−1.06	1.13E+01
232677_at	AU146128	SYT11	EC	−4.22	3.62E−04	−1.78	2.27E−02
209198_s_at	BC004291	SYT11	VCX	1.24	8.14E−03	1.05	4.00E+00
228072_at	AK024280	SYT12	EC	−3.53	2.73E−04	−1.82	1.07E−02
226086_at	AB037848	SYT13	HIP	−2.77	1.87E−04	−2.28	1.64E−04
205613_at	NM 016524	SYT17	EC	−3.87	6.19E−04	−2.24	5.66E−03
205613_at	NM 016524	SYT17	MTG	−1.94	7.35E−03	1.09	1.86E+00
205613_at	NM 016524	SYT17	VCX	−2.66	4.87E−04	1.67	6.60E−03
213326_at	AU150319	VAMP1	VCX	1.52	2.61E−04	−1.38	8.47E−02
201556_s_at	BC002737	VAMP2	EC	−4.27	2.82E−05	−1.63	1.62E−02
214792_x_at	AI955119	VAMP2	EC	−6.32	1.18E−05	−1.65	3.07E−02
201556_s_at	BC002737	VAMP2	SFG	−2.94	8.11E−03	−3.78	4.04E−03
201336_at	BC003570	VAMP3	HIP	−2.02	1.18E−03	−1.36	2.88E−01
201336_at	BC003570	VAMP3	MTG	−2.21	1.06E−03	1.12	1.82E+00
201336_at	BC003570	VAMP3	PC	−1.76	7.18E−03	−1.25	1.14E+00
213480_at	AF052100	VAMP4	MTG	1.96	1.93E−04	1.28	1.39E−01
213480_at	AF052100	VAMP4	VCX	1.54	2.40E−03	−1.40	3.66E−02

* Corrected *P* values are shown.

Table 4

Unique expression changes in NDAD brains

Probe set ID	Genbank ID	Gene symbol	Brain region	NDAD vs. control	
				Fold	*P*-value*
225112_at	AA058571	ABI2	HIP	1.33	5.12E−03
225098_at	BF245400	ABI2	HIP	2.27	2.41E−04
225098_at	BF245400	ABI2	MTG	1.70	3.66E−05
203381_s_at	N33009	APOE	EC	−3.45	5.18E−03
203382_s_at	NM 000041	APOE	EC	−4.35	6.54E−04
212884_x_at	AI358867	APOE	EC	−5.01	1.46E−04
203382_s_at	NM 000041	APOE	HIP	−2.40	3.82E−03
212884_x_at	AI358867	APOE	HIP	−2.26	1.23E−03
203381_s_at	N33009	APOE	HIP	−5.05	5.36E−04
203381_s_at	N33009	APOE	MTG	−2.75	9.06E−04
203382_s_at	NM 000041	APOE	MTG	−3.00	1.44E−04
212884_x_at	AI358867	APOE	MTG	−2.58	2.07E−05
212884_x_at	AI358867	APOE	PC	−2.02	2.40E−03
203381_s_at	N33009	APOE	PC	−2.47	1.52E−03
204065_at	NM 004854	CHST10	HIP	−1.95	5.45E−03
209618_at	U96136	CTNND2	HIP	−1.71	2.92E−03
209618_at	U96136	CTNND2	MTG	−1.64	5.90E−03
202668_at	BF001670	EFNB2	HIP	1.97	1.86E−03
227404_s_at	AI459194	EGR1	EC	−2.07	1.04E−03
201693_s_at	AV733950	EGR1	EC	−3.14	1.60E−04
227404_s_at	AI459194	EGR1	PC	−1.99	2.52E−03
216033_s_at	S74774	FYN	EC	−3.26	6.07E−03
210105_s_at	M14333	FYN	EC	−3.04	4.41E−07
216033_s_at	S74774	FYN	HIP	−2.73	6.50E−03
216033_s_at	S74774	FYN	MTG	−2.85	2.20E−03
212737_at	AL513583	GM2A	EC	−2.43	5.07E−03
212737_at	AL513583	GM2A	MTG	−1.69	7.63E−03

Probe set ID	Genbank ID	Gene symbol	Brain region	NDAD vs. control	
				Fold	*P*-value*
35820_at	M76477	GM2A	MTG	−1.98	5.17E−03
212737_at	AL513583	GM2A	PC	−1.78	3.97E−03
207548_at	NM 000844	GRM7	MTG	1.79	8.18E−05
236437_at	N30158	LAMB1	MTG	2.53	1.82E−04
206401_s_at	J03778	MAPT	HIP	2.73	7.86E−03
203928_x_at	AI870749	MAPT	HIP	2.48	5.15E−04
225379_at	AA199717	MAPT	HIP	−2.40	6.12E−05
225379_at	AA199717	MAPT	MTG	−2.00	7.44E−03
203928_x_at	AI870749	MAPT	MTG	2.16	8.61E−04
203928_x_at	AI870749	MAPT	PC	1.90	4.89E−03
202742_s_at	NM 002731	PRKACB	MTG	3.74	7.08E−05
227817_at	R51324	PRKCB1	EC	−2.54	7.99E−04
228795_at	AI523569	PRKCB1	EC	−2.08	4.55E−04
209465_x_at	AL565812	PTN	EC	−2.16	1.48E−03
209466_x_at	M57399	PTN	EC	−3.87	8.75E−04
211737_x_at	BC005916	PTN	EC	−4.55	1.68E−04
211737_x_at	BC005916	PTN	PC	−2.22	4.62E−03
209466_x_at	M57399	PTN	PC	−2.51	2.51E−03
209465_x_at	AL565812	PTN	SFG	−2.79	1.00E−03
209686_at	BC001766	S100B	PC	−2.46	4.52E−04
206330_s_at	NM 016848	SHC3	HIP	−1.72	9.61E−04
208845_at	BC002456	VDAC3	MTG	1.57	6.31E−03

*Corrected *P* values are shown.

Table 5

Regional principal components analysis

Brain region	Probe set ID	Genbank ID	Gene symbol	Brain region	Probe set ID	Genbank ID	Gene symbol
EC	200766_at	NM 001909	CTSD	MTG	213347_x_at	AW132023	RPS4X
EC	204212_at	NM 005469	ACOT8	MTG	232160_s_at	AL137262	TNIP2
EC	227876_at	AW007189	KIAA1688	MTG	225782_at	AW027333	MSRB3
EC	218580_x_at	NM 017900	AURKAIP1	MTG	212377_s_at	AU158495	NOTCH2
EC	1558102_at	AK055438	TM6SF1	MTG	228214_at	AW242286	SOX6
EC	208977_x_at	BC004188	TUBB2	MTG	226913_s_at	BF527050	SOX8
EC	212085_at	AA916851	SLC25A6	MTG	211962_s_at	BG250310	ZFP36L1
EC	1555740_a_at	AF483549	MRAP	MTG	240648_at	AW104578	LOC440728
EC	238528_at	AI361043	UBR1	MTG	204906_at	BC002363	RPS6KA2
EC	209914_s_at	AW149405	NRXN1	MTG	212923_s_at	AK024828	C6orf145
EC	204143_s_at	NM 017512	ENOSF1	PC	226031_at	AA523733	FLJ20097
EC	223319_at	AF272663	GPHN	PC	218877_s_at	NM 021820	C6orf75
EC	210998_s_at	M77227	HGF	PC	206833_s_at	NM 001108	ACYP2
EC	1567374_at	AJ011596		PC	238206_at	AI089319	
EC	202192_s_at	NM 005890	GAS7	PC	222975_s_at	AI423180	CSDE1
EC	204120_s_at	NM 001123	ADK	PC	235195_at	BG109988	FBXW2
HIP	217740_x_at	NM 000972	RPL7A	PC	240748_at	AI939338	
HIP	203865_s_at	NM 015833	ADARB1	PC	208880_s_at	AB019219	C20orf14
HIP	206491_s_at	NM 003827	NAPA	PC	201678_s_at	NM 020187	DC12
HIP	206457_s_at	NM 000792	DIO1	PC	217452_s_at	Y15014	B3GALT2
HIP	227144_at	AA476916	C22orf9	PC	222627_at	AK002205	VPS54
HIP	222505_at	BF510801	LMBR1	PC	53071_s_at	AI885411	FLJ22222
HIP	201386_s_at	AF279891	DHX15	PC	218125_s_at	NM 018246	CCDC25
HIP	224606_at	BG250721	KLF6	PC	213535_s_at	AA910614	UBE2I
HIP	217792_at	NM 014426	SNX5	PC	222459_at	BG109865	C1orf108
HIP	200822_x_at	NM 000365	TPI1	PC	223093_at	T99215	ANKH
HIP	204701_s_at	NM 004809	STOML1	PC	219248_at	NM 025264	THUMPD2
HIP	203522_at	NM 005125	CCS	PC	226650_at	AI984061	ZFAND2A
HIP	225077_at	AA890703	LOC283680	PC	225018_at	BF512188	SPIRE1

Brain region	Probe set ID	Genbank ID	Gene symbol	Brain region	Probe set ID	Genbank ID	Gene symbol
HIP	223313_s_at	BC001207	MAGED4	PC	214257_s_at	AA890010	SEC22L1
HIP	202282_at	NM 004493	HADH2	PC	218771_at	NM 018216	PANK4
HIP	1568698_at	BC042563		PC	208826_x_at	U27143	HINT1
HIP	203081_at	NM 020248	CTNNBIP1	PC	227797_x_at	AI652464	DJ122O8.2
HIP	201155_s_at	NM 014874	MFN2	PC	215093_at	U82671	NSDHL
HIP	209178_at	AF038391	DHX38	PC	219288_at	NM 020685	C3orf14
HIP	201956_s_at	NM 014236	GNPAT	PC	207573_x_at	NM 006476	ATP5L
HIP	200001_at	NM 001749	CAPNS1	SFG	202936_s_at	NM 000346	SOX9
HIP	234813_at	AB051477	MGC3040	SFG	208623_s_at	J05021	VIL2
HIP	201144_s_at	NM 004094	EIF2S1	SFG	205608_s_at	U83508	ANGPT1
HIP	222443_s_at	AF182415	RBM8A	SFG	224565_at	BE675516	TncRNA
HIP	227880_s_at	AW300965	FAM11A	VCX	1555876_at	BG290185	
HIP	216032_s_at	AF091085	C20orf47	VCX	237931_at	AI732263	
HIP	200017_at	NM 002954	RPS27A	VCX	211384_s_at	D50855	CASR
HIP	1553101_a_at	NM 017758	FLJ20308	VCX	210640_s_at	U63917	GPR30

Genes correlating with component 1 (correlation = 1) for each regional analysis are listed.

Table 6

RT-PCR validation of selected genes

Probe set ID	Gene name	GenBankID	MTG-array data				MTG-RT-PCR data						
			NDAD/control		AD/control		Normalized fold			NDAD/control fold change	NDAD/control *t*-test *P*-value	AD/control fold change	AD/control *t*-test *P*-value
			Fold change	Corrected *P*-value	Fold change	Corrected *P*-value	Control	NDAD	AD				
209793_at	GRIA1	AL567302	−1.42	3.44E−02	−2.57	2.86E−06	1.00	0.26	0.39	−3.85	3.61E−04	−2.56	6.88E−03
208032_s_at	GRIA3	NM_000828	2.04	1.19E−02	−1.27	3.36E−01	1.00	0.53	0.37	−1.89	4.93E−02	−2.70	1.63E−02
217506_at	GRIA3	BF110551	3.21	7.79E−03	1.19	2.16E+00							
206732_at	GRIA3	NM_007325	3.67	1.85E−04	1.82	3.34E−02							
1569280_s_at	GRIA3	BC032004	2.15	1.10E−04	−1.32	1.44E+00							
214517_at	MAP1B	BG164365	2.45	4.30E−03	1.76	1.71E−01	1.00	0.84	0.43	−1.19	3.85E−01	−2.33	5.46E−03
212233_at	MAP1B	AL523076	−2.27	1.07E−05	−4.27	2.21E−07							
203381_s_at	APOE	N33009	−2.75	9.06E−04	1.89	2.34E−02	1.00	0.59	0.54	−1.69	2.55E−04	−1.85	2.47E−03
203382_s_at	APOE	NM_000041	−3.00	1.44E−04	1.53	1.08E−02							
212884_x_at	APOE	AI358867	−2.58	2.07E−05	1.80	8.77E−04							
214953_s_at	APP	X06989	2.37	1.35E−03	1.12	1.44E+00	1.00	0.47	0.45	−2.13	1.59E−03	−2.22	6.40E−03
200602_at	APP	NM_000484	5.11	6.71E−04	3.09	8.20E−07							
231087_at	BACE1	BF939127	−1.47	4.08E−02	−1.26	3.27E−01	1.00	0.38	0.55	−2.63	3.51E−03	−1.82	3.96E−02
217904_s_at	BACE1	NM_012104	−1.75	9.56E−06	−1.32	2.58E−03							
213735_at	COX5B	AI557312	−4.20	9.44E−04	−4.43	9.31E−04	1.00	0.30	0.43	−3.33	1.05E−06	−2.33	4.39E−03
211022_x_at	COX5B	BC006229	−2.97	6.05E−04	−3.34	3.64E−04							
202343_x_at	COX5B	NM_001862	−2.75	1.72E−04	−2.94	1.35E−04							
213735_s_at	COX5B	AI557312	−2.03	8.57E−05	−2.21	2.25E−05							
212567_s_at	MAP4	AL523310	−1.80	1.75E−02	2.40	1.60E−03	1.00	0.56	0.7	−1.79	3.54E−03	−1.43	2.68E−02
33850_at	MAP4	W28892	−1.70	9.05E−03	2.50	3.75E−03							
Probe set ID	Gene name	GenBank ID	PC-array data				PC-RT-PCR data						
			NDAD/control		AD/control		Normalized fold			NDAD/control fold change	NDAD/control *t*-test *P*-value	AD/control fold change	AD/control *t*-test *P*-value
			Fold change	Corrected *P*-value	Fold change	Corrected *P*-value	Control	NDAD	AD				
203381_s_at	APOE	N33009	−2.47	1.52E−03	−2.57	7.47E−04	1.00	0.64	0.73	−1.56	2.35E−03	−1.37	1.47E−02

Probe set ID	Gene name	GenBankID	MTG-array data				MTG-RT-PCR data						
			NDAD/control		AD/control		Normalized fold			NDAD/control fold change	NDAD/control *t*-test *P*-value	AD/control fold change	AD/control *t*-test *P*-value
			Fold change	Corrected *P*-value	Fold change	Corrected *P*-value	Control	NDAD	AD				
203382_s_at	APOE	NM_000041	−1.94	2.35E−02	−1.25	8.31E−01							
212884_x_at	APOE	AI358867	−2.02	2.40E−03	−1.22	5.71E−01							
211277_x_at	APP	BC004369	1.69	4.54E−04	3.01	2.05E−04	1.00	0.51	0.74	−1.96	9.95E−03	−1.35	1.33E−01
200602_at	APP	NM_000484	2.11	1.87E−04	1.93	8.38E−04							
222460_s _at	BACE1	AI653425	−1.34	3.96E−02	−1.17	9.87E−01	1.00	0.40	0.56	−2.50	2.58E−02	−1.79	5.22E−02
222461_s _at	BACE1	AF190725	−2.05	1.62E−04	−1.16	1.12E+00							
231088_at	BACE1	BF939127	−1.57	3.81E−03	−1.35	3.27E−01							
211025_x_at	COX5B	BC006229	−2.08	2.39E−03	−3.68	1.55E−05	1.00	0.32	0.68	−3.13	2.22E−06	−1.47	2.84E−02
202336_x_at	COX5B	NM_001862	−2.18	3.87E−03	−4.08	1.44E−05							
235063_at	MAP4	AI078534	1.75	2.89E−02	−2.17	3.05E−02	1.00	0.60	0.84	−1.67	3.96E−04	−1.19	3.06E−01

RT-PCR validation data for the MTG and PC of unprofiled controls, NDAD cases, and AD cases are shown. Corresponding microarray expression data are also listed.

Neurobiol Aging. Author manuscript; available in PMC 2010 April 1.